Discriminating fluvial fans and deltas: Channel network morphometrics reflect distinct formative processes

Luke Gezovich[1*], Piret Plink-Björklund[1], Jack Henry[1,2]
[1] Colorado School of Mines, Geology & Geologic Engineering, 1500 Illinois Street, Golden, CO, 80401
[2] Rice University, Earth, Environmental and Planetary Sciences, 6100 Main St., Houston, TX, 77005-1827

Correspondence to: Luke Gezovich (lukegezovich@mines.edu)

Abstract

Recent recognition of a new type of fluvial system – fluvial fans – introduces a fan-shaped channel network that appears similar to that of river-dominated deltas. Deltas form where rivers enter lakes and oceans, while fluvial fans are terrestrial landforms. However, fluvial fans can reach the shorelines of oceans or lakes, and in such cases the distinction between fluvial fan and river-dominated delta channel networks becomes ambiguous. We currently lack fundamental understanding of these two landforms' morphometric differences, despite their high socioeconomic significance, vulnerability to natural hazards, and key differences in how these landforms respond to global climate change and urbanization. Here we review the relevant conceptual differences in delta and fluvial fan network morphodynamics, propose a set of quantitative morphometric criteria to distinguish fluvial fan and delta channel networks, and test these criteria on 40 deltas and 40 fluvial fans from across the world. This initial attempt to contrast and distinguish deltas and fluvial fans based on their channel network morphometrics demonstrates that quantifying channel network angles (mean of 73.8° for deltas and 55.0° for fluvial fans) and trends in normalized channel widths and lengths provide efficient criteria, but some ambiguities remain that need to be resolved in future work. This research advances our mechanistic understanding of fluvial fan and delta channel networks and the recognition of modern and ancient landforms on Earth and other planetary bodies, such as Mars and Saturn's moon Titan.

Plain Language Summary

Fluvial fans are a newly recognized type of river system that look like river deltas, especially when they reach lakes or oceans. This study explores how to tell them apart by measuring the size and layout of channels in these fan-shaped landforms. Understanding these differences helps to predict how these landforms respond to climate change and urbanization, and to identify them on Mars and other planetary bodies.

1. Introduction

River deltas are depositional landforms that form where rivers enter lakes or oceans. They are home to over half a billion people, host abundant and biodiverse ecosystems, and function as both economic and agricultural hubs (Saito et al., 2007; Tejedor et al., 2015). Deltas are global change hotspots highly vulnerable to urbanization and climate change, which can aggravate coastal hazards and cause sea level rise (Giosan et al., 2014; Syvitski et al., 2009), and reduce sediment supply due to river damming and artificial levees, causing the drowning of deltas (Blum & Roberts, 2009; Giosan et al., 2014; Nienhuis et al., 2020; Paola et al., 2011; Syvitski et al., 2009). The form and function of deltas is intimately linked to the evolving structure of their channel networks that determine how deltas distribute sediment and nutrients (Passalacqua, 2017; Pearson et al., 2020; Tejedor et al., 2017). Delta channel network morphology results from an intricate balance between sediment erosion and deposition from river, tide, and wave energy fluxes. River fluxes create distributary channels and islands, tides roughen the shoreline and widen the channels, and waves smooth the shoreline and decrease the number of distributary channels (Broaddus et al., 2022; Galloway, 1975; Nienhuis et al., 2015, 2018; Paniagua-Arroyave & Nienhuis, 2024; Vulis et al., 2023). Deltas dominated by river energy fluxes (river-dominated deltas) (Broaddus et al., 2022; Galloway, 1975; Nienhuis et al., 2015, 2018; Paniagua-Arroyave & Nienhuis, 2024; Vulis et al., 2023) characteristically form fan-shaped landforms with complex distributary channel networks (Fig. 1). In these deltas, channel network topology is defined by mouth bar deposition and consequent distributary channel bifurcation (Bates, 1953; Edmonds & Slingerland, 2007; Wright, 1977).

Fluvial fans are another type of fan-shaped landform with channel networks that share morphological similarities with the river-dominated delta channel networks (Fig. 2). Fluvial fans are a relatively newly acknowledged type of fluvial landform (Ventra & Clarke, 2018; Weissman et al., 2010), which forms via river avulsions or "channel jumps" across low-gradient floodplains (Chakraborty et al., 2010; Martin & Edmonds, 2023; North & Warwick, 2007). Rivers have been traditionally regarded as sediment transfer or bypass zones in source-to-sink systems (Allen, 2008; Fielding et al., 2012), whereas fluvial fans are net depositional and build significant stratigraphic thicknesses (Chakraborty et al., 2010; Moscariello, 2018; Weissmann et al., 2015). Fluvial fans are also called "wet" fluvial-dominated alluvial fans (Schumm, 1977), megafans (Singh et al., 1993), or distributive fluvial systems (DFS) (Weissman et al., 2010). Fluvial fans are distinct landforms from alluvial fans – which form by a combination of gravitational and streamflow processes, feature steep gradients (typically 2–12°), and have a relatively small radius typically less than 10 km (Blair & McPherson, 1994; Moscariello, 2018). Fluvial fans form some of the largest terrestrial landforms on Earth (10^3–10^5 km^2 in surface area) (Horton & Decelles, 2001; Leier et al., 2005) and have low gradients (0.0018–1.5°) (Hartley et al., 2010). Fluvial fans are abundant

Moved (insertion) [3]

Commented [PP1]: This sentence was out of place below

Deleted: To specifically refer to these deltaic processes, we define "bifurcations" as a process related to mouth bar deposition and consequent channel branching.

Commented [LG2]: We originally had a range from Brooke et al., 2022 but I replaced it with this because their value range is fans to fan-deltas, while this represents the whole range from Hartley's more comprehensive database

Commented [PP3R2]: I am getting confused between the two manuscripts.... I think it is ok to just have this reference here

Deleted: typically

Deleted: 0.03–0.001°

across Earth, and they form in diverse climatic and tectonic settings (Hartley et al., 2010; Ventra & Clarke, 2018; Weissmann et al., 2010).

Like deltas, fluvial fans are home to hundreds of millions of people, and these highly dynamic landforms are critical for their livelihood – supporting agriculture, fisheries, and freshwater access. They also experience catastrophic floods; for example, the Kosi fluvial fan floods have led to large numbers of casualties and displaced populations (Sinha, 2009; Syvitski & Brakenridge, 2013). While fluvial fans are terrestrial landforms, they can reach the shorelines of oceans (Fig. 2b) or lakes (Figs. 2a, 2d and 2i). In such cases the distinction between fluvial fan and river-dominated delta channel networks becomes ambiguous, while wave- and tide-dominated deltas have distinctly recognizable morphologies (Broaddus et al., 2022; Galloway, 1975; Nienhuis et al., 2015; 2018; Paniagua-Arroyave & Nienhuis, 2024; Vulis et al., 2023). We currently lack quantitative morphometric criteria for distinguishing river-dominated delta and fluvial fan channel networks, despite their socioeconomic significance, key differences in their natural hazard vulnerabilities, and in how they respond to global change.

Numerous fan-shaped landforms with channel networks have also been identified on other planetary bodies such as Mars (Malin & Edgett, 2015; Ori et al., 2000; Wood, 2006) and Saturn's moon Titan (Radebaugh et al., 2018; Wall et al., 2010; Witek & Czechowski, 2015). Deltas on planetary bodies are important indicators of paleo-shorelines and have been utilized to reconstruct the shorelines and water levels of ancient lakes and oceans on Mars (Di Achille & Hynek, 2010). However, Martian paleo-ocean shoreline reconstructions have so far yielded mixed results (De Toffoli et al., 2021). This discrepancy could perhaps arise because shoreline-bound deltas have not been effectively distinguished from fluvial fans on Mars, which may form thousands of kilometers inland from shorelines (Bramble et al., 2019; Limaye et al., 2023; Tebolt & Goudge, 2022). Deltas also offer attractive targets for mission sites in search of life due to their habitability and high biosignature preservation potential, as exemplified by the selection of Jezero Crater for NASA's *Perseverance* rover, *Ingenuity* helicopter, and future Mars Sample Return mission (Farley et al., 2020). Distinguishing deltaic and fluvial fan paleo-channel networks on other planetary bodies is even more ambiguous, especially if the lakes and oceans are no longer present.

Over time, the accumulation of biogenic and sedimentary materials distributed via channel networks contributes to the construction of stratigraphy. Fluvial fans and deltas are both net depositional systems characterized by spatially diminishing water surface slopes that reduce sediment transport capacity, thereby producing spatiotemporal convergence and deposition of sediment (Ganti et al., 2014). Consequently, in addition to their socioeconomic significance, both landforms significantly contribute to the stratigraphic record, and their deposits can be used to decipher past environmental conditions. High deposition rates in fluvial fans and deltas promote the preservation of environmental change signals in the sedimentary record (Trampush & Hajek, 2017). Similar to modern river-dominated deltas and fluvial

Deleted: .

Deleted: F

Deleted: experiences catastrophic river

Deleted: that

Deleted: lead

Moved up [3]: Deltas are global change hotspots highly vulnerable to urbanization and climate change, which can aggravate coastal hazards and cause sea level rise (Giosan et al., 2014; Syvitski et al., 2009), and reduce sediment supply due to river damming and artificial levees, causing the drowning of deltas (Blum & Roberts, 2009; Giosan et al., 2014; Nienhuis et al., 2020; Paola et al., 2011; Syvitski et al., 2009).

Deleted: ,

Deleted: as both are

fans, we lack morphometric criteria to distinguish these two fan-shaped channel networks in the sedimentary record, such as in seismic datasets.

This study is motivated by developing quantitative morphometric distinction criteria for fluvial fan and river-dominated delta channel networks. Prior work has established quantitative morphological criteria for describing deltaic channel networks and linked these characteristics to theory (Chen et al., 2021; Coffey & Shaw, 2017; Edmonds et al., 2011; Edmonds & Slingerland, 2007; Fagherazzi et al., 2015; Ke et al., 2019; Passalacqua, 2017; Pearson et al., 2020; Tejedor et al., 2015, 2017). However, there are no existing quantitative criteria to characterize fluvial fan channel networks or to differentiate the two landforms. To develop such criteria, we review the relevant conceptual differences in delta and fluvial fan network morphodynamics, propose quantitative morphometric criteria to distinguish fluvial fan and delta channel networks, and test these criteria on 40 deltas and 40 fluvial fans (Supplementary Data) from across the globe (Fig. 3). We test the robustness of the approach by analyzing differences in channel network morphometrics concerning the size and gradient of the systems, lake versus ocean terminations and tide versus wave influences in deltas, and fan termination styles in fluvial fans. We assess how effectively the proposed methods distinguish fluvial fans from river-dominated deltas and examine why this distinction matters under global change. This work serves to improve our mechanistic understanding of fluvial fan and delta evolution, and their accurate recognition on Earth, other planetary bodies, and in the sedimentary record.

Deleted: , hydroclimate conditions

Deleted: channel

Deleted: morphology

2. Delta and Fluvial Fan Channel Network Morphodynamics

The nature of channel networks is dependent on distinct morphodynamic processes responsible for their formation (Edmonds & Slingerland, 2007; Fagherazzi et al., 2015; Tejedor et al., 2015). Below we analyze differences in delta and fluvial fan morphodynamics and review existing morphometric criteria for quantifying deltaic distributary channel networks. Our review is not comprehensive; rather, it focuses on the specific processes that govern the formation of the morphometric characteristics that we can then use for distinction of these two landforms, namely channel network angles, and downstream changes in channel widths and lengths. There are other important characteristics of deltaic channel networks, linked to water and sediment discharge distribution, entropy, and connectivity (Chen et al., 2021; Ke et al., 2019; Passalacqua, 2017; Pearson et al., 2020; Tejedor et al., 2015, 2017). These aspects are not considered in this review, because they are outside the scope of this study that seeks to distinguish deltaic and fluvial fan channel networks using easily applicable morphometric criteria that can be used for both deltaic and fluvial fan networks.

2.1 River Deltas

Deltas (Fig. 1) form only where a river enters a standing body of water. Here, the transport capacity of the turbulent jet decreases, and the "parent" stream jet flow experiences both lateral and bed friction,

Deleted: We use the terms bifurcation and avulsion as *processes* rather than a geomorphological feature of channel splitting. *Bifurcation* is the process of channel splitting driven by mouth bar formation (Edmonds & Slingerland, 2007). *Avulsions* are channel "jumps", where a channel changes its course due to channel superelevation or a more favorable (steeper) gradient at channel flanks (Gearon et al., 2024; Jones & Schumm, 1999; Slingerland & Smith, 2004). Partial avulsions can result in two downstream channels which both convey dischargesplit channels; however, the avulsion process here is distinct from channel *bifurcation* around at a mouth bar.¶

causing the flow to decelerate and rapidly expand laterally (Bates, 1953; Edmonds & Slingerland, 2007; Jerolmack & Swenson, 2007; Wright, 1977). As a result, the transport capacity of the turbulent jet decreases and sediment is deposited as a mouth bar basinward of the river mouth (Edmonds & Slingerland, 2007). The process of mouth bar deposition and growth eventually leads to the downstream branching, or *bifurcation*, of a single (parent) channel into two daughter channels (Axelsson, 1967; Coffey & Shaw, 2017; Edmonds & Slingerland, 2007) (Fig. 4a). These daughter channels are separated by an island or shallow bay where sediment transport is significantly reduced or nonexistent, and flow is unchannelized (Coffey & Shaw, 2017). Mouth bar deposition and resultant channel bifurcation repeat multiple times, leading to the seaward advancement of the shoreline and the construction of a delta distributary channel network (Edmonds & Slingerland, 2007; Olariu & Bhattacharya, 2006) (Fig. 4a).

Deltas also experience channel avulsions or "channel jumps" at the lobe-level (Slingerland & Smith, 2004). These deltaic avulsions occur within a region of high-water surface slope variability caused by backwater hydrodynamics that are characterized by spatial flow deceleration and deposition during low flows, and flow acceleration and bed scour with high flows (Brooke et al., 2022; Chatanantavet et al., 2012; Chatanantavet & Lamb, 2014). As the backwater zone sets the location for avulsion in deltas (Chatanantavet et al., 2012), they are strongly controlled by hydrodynamics in their receiving basin, like mouth-bar-driven bifurcations. As a result, the delta lobe size is generally consistent and the lobe avulsion node migrates downstream commensurate with shoreline progradation (Ganti et al., 2014), as influenced by flood frequency, sediment supply, or sea-level rise (Brooke et al., 2022). These avulsions episodically rearrange the depocenter at the delta lobe scale, whereas the substantially more frequent mouth-bar-driven bifurcations generate the topology of the delta distributary channel networks (Bentley et al., 2016; Edmonds & Slingerland, 2007).

Resultant delta channel networks have a specific angle at which distributary channels bifurcate (Fig. 4a) (Coffey & Shaw, 2017), because a mouth-bar-driven bifurcation will grow toward an equilibrium angle of 72° to maximize flux at the two channel tips (Coffey & Shaw, 2017; Devauchelle et al., 2012; Ke et al., 2019; Mahon et al., 2024). First described in tributary networks, this theoretical angle arises from diffusive groundwater flow (Devauchelle et al., 2012). Testing of this concept reports mouth-bar-driven bifurcation angles of 70.4° ± 2.6° (n = 9) in natural deltas (Coffey & Shaw, 2017), and 68.3° ± 8.7° (n = 21) (Coffey & Shaw, 2017) and 74.1° ± 7.7° (n = 13) (Federici & Paola, 2003) in experimental deltas.

Deltaic channel networks tend to consistently self-organize (Edmonds et al., 2011; Fagherazzi, 2008) and exhibit a theoretical fractal pattern of decreasing channel widths and lengths associated with increasing bifurcation order (Edmonds et al., 2011; Edmonds & Slingerland, 2007; Hariharan et al., 2022; Seybold et al., 2017; Wolinsky et al., 2010) (Fig. 4a). Edmonds & Slingerland, (2007) show that channel width trends align with hydraulic geometric scaling: as the discharge of a parent channel divides into the

Deleted: bifurcation, or

Deleted:

Formatted: Font: Italic

Deleted: channel

discharge for two resultant daughter channels, the daughter channel dimensions decrease as they scale with bankfull discharge. Channel lengths decrease downstream with each successive bifurcation because the jet momentum flux and consequent average grain transport distance decrease downstream, causing new mouth bar deposition and accompanying bifurcations to occur closer to the previous bifurcation node for a given channel (Edmonds & Slingerland, 2007) (Figs. 4a).

The nature of delta channel networks is further affected by waves and tides (Broaddus et al., 2022; Geleynse et al., 2011; Jerolmack & Swenson, 2007) where the relative strength of river, wave, and tide processes determines whether deltas are river, wave, or tide dominated (Galloway, 1975; Nienhuis et al., 2015, 2018; Paniagua-Arroyave & Nienhuis, 2024; Vulis et al., 2023). Since wave- and tide-*dominated* deltas exhibit distinct morphologies from river-dominated delta and fluvial fan channel networks, they are not considered in this study (See Methods for more information on classification).

Deleted: and 5a

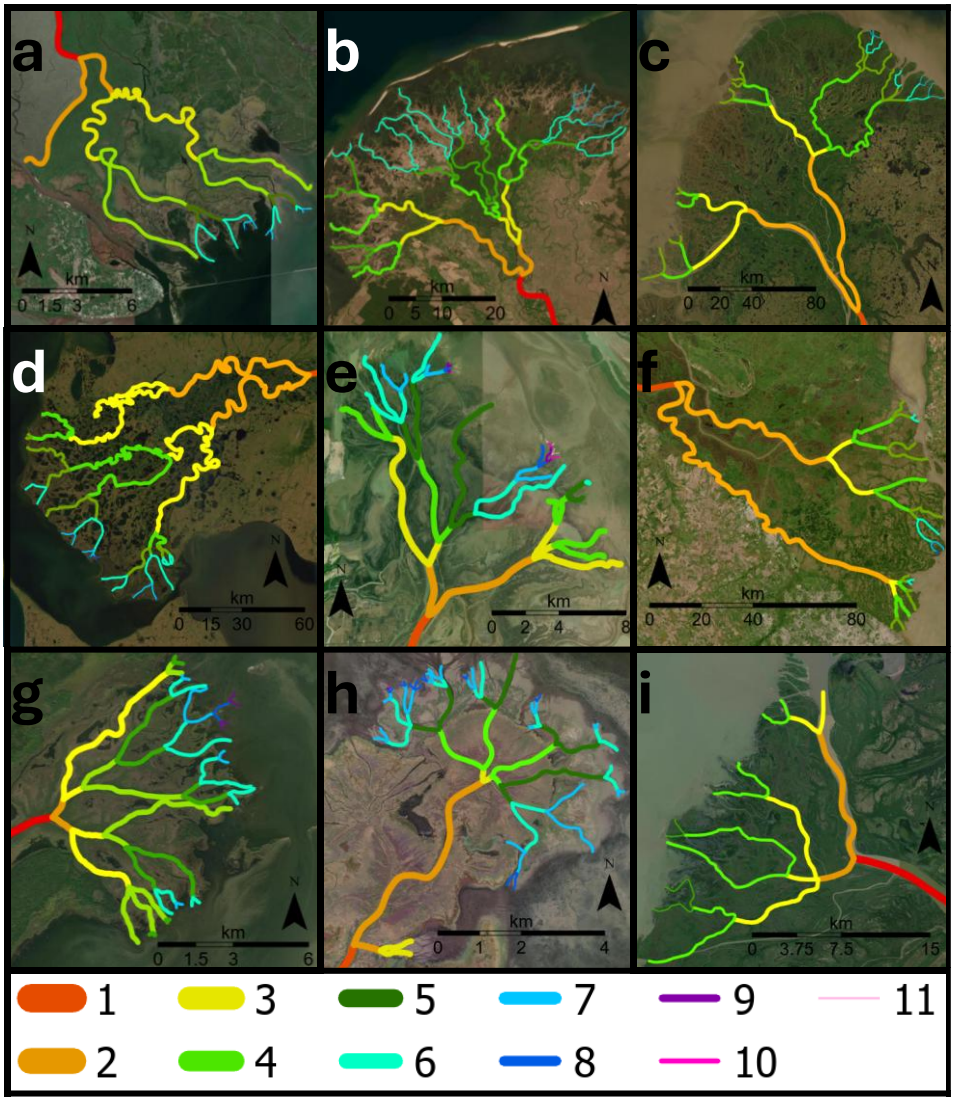

Figure 1: Examples of delta channel networks: (a) Apalachicola, (b) Selenga, (c) Yukon, (d) Kobuk, (e) Poyang Lake, (f) Parana (g) Saskatchewan, (h) Mamawi lake, (i) Slave deltas. The colors indicate channel hierarchy (see Methods). Base imagery from Esri's World Imagery basemap (© Esri, DigitalGlobe, GeoEye, i-cubed, USDA FSA, USGS, AEX, Getmapping, Aerogrid, IGN, IGP, swisstopo, and the GIS User Community). Colors and relative line thicknesses indicate channel hierarchy (see Methods), with the widest lines representing order 1 channels and progressively thinner lines representing higher channel orders.

236

2.2 Fluvial Fans

Fluvial fans are fan-shaped landforms that form by river avulsions or "channel jumps" across a low-gradient floodplain (Chakraborty et al., 2010; Martin & Edmonds, 2023). In contrast to deltas where mouth-bar-driven bifurcations and backwater-driven avulsions are strongly controlled by hydrodynamics near a receiving basin of standing water (Brooke et al., 2022; Chatanantavet et al., 2012; Ganti et al., 2014), *avulsions* that form fluvial fans are driven by a topographic slope break (Ganti et al., 2014; Martin & Edmonds, 2023). Increased likelihood of avulsions at the fan apex is a consequence of the gradient reduction that triggers in-channel sediment aggradation (Parker et al., 1998). These avulsions result from high channel bed aggradation rates that are considerably higher than on the surrounding floodplains (Pizzuto, 1987). Set up by in-channel aggradation, avulsions develop where a channel changes its course due to channel superelevation (Bryant et al., 1995; Gearon et al., 2024; Mohrig et al., 2000) or a more favorable (steeper) gradient at channel flanks (Gearon et al., 2024; Jones & Schumm, 1999; Slingerland & Smith, 2004). Since the slope break controls the location of the fluvial fan's apex, this avulsion node is topographically pinned at this change in gradient, unlike in deltas (Ganti et al., 2014; Brooke et al., 2022). Partial or full avulsions also occur further downfan, involving local gradient or discharge decreases, or crevassing processes (Assine, 2005; Chakraborty et al., 2010; Donselaar et al., 2013; Gearon et al., 2024) (Fig. 2).

Fluvial fan channel networks thus result through repeated nodal style avulsions (Slingerland & Smith, 2004) that typically shift the primary river to different regions of the fan (Chakraborty et al., 2010; Martin & Edmonds, 2023; North & Warwick, 2007). These avulsions superimpose new channel positions on paleo-channel locations and can split channels by partial avulsions and crevasses. This generates channel and paleo-channel branching formed by processes distinct from deltas (North & Warwick, 2007) (Fig. 4b), where channel branching is predominantly caused by mouth-bar-driven bifurcations. In fluvial fans, channel branching is related to avulsions, which generate channel networks that are predominantly paleo-channel networks rather than active channel networks like in deltas (Chakraborty et al., 2010; North & Warwick, 2007). Multiple channels can actively transmit discharge at partial avulsions, such as during major river floods.

Downfan decreases in channel width have been well documented in modern and ancient fluvial fans (Davidson et al., 2013; Kelly & Olsen, 1993; Nichols, 1987; Nichols & Fisher, 2007; Owen et al., 2015; Wang & Plink-Björklund, 2019; Weissman et al., 2010), linked to discharge losses to floodplain processes, infiltration into the loose sediments of the fan, and evapotranspiration (Davidson et al., 2013; Hartley et al., 2010; Horton & Decelles, 2001; Weissman et al., 2010). However, some fluvial fan channels have also been shown to widen downstream, possibly due to changes in channel planform or aspect ratio, discharge contribution from groundwater, or discharge capture from adjacent rivers

Deleted: fluvial fan river

Formatted: Font: Italic

Deleted: This process causes river channel superelevation which ultimately triggers river avulsions near the fan apex (Bryant et al., 1995; Gearon et al., 2024; Mohrig et al., 2000). …

Deleted: this

Deleted: the

Deleted: thus

Deleted: (Ganti et al., 2014)

Deleted: abrupt

Deleted: do

Deleted: (Slingerland & Smith, 2004)

Deleted: to

Deleted: apparent channel "bifurcations"

Deleted: . However, as a process, these are not bifurcations related to mouth bar deposition but rather generated by avulsions…

Deleted: s. Furthermore, fluvial fan

(Chakraborty et al., 2010; Davidson et al., 2013). Fluvial fan channel networks have been studied for qualitative descriptions of channel planform morphology (Davidson et al., 2013; Hartley et al., 2010; Weissman et al., 2010) and scaling relationships (Davidson et al., 2013; Davidson & Hartley, 2014). Modeling establishes a relationship between the fluvial fan shape and avulsion dynamics, like avulsion trigger period and abandoned channel dynamics (Edmonds et al., 2022; Martin & Edmonds, 2023).

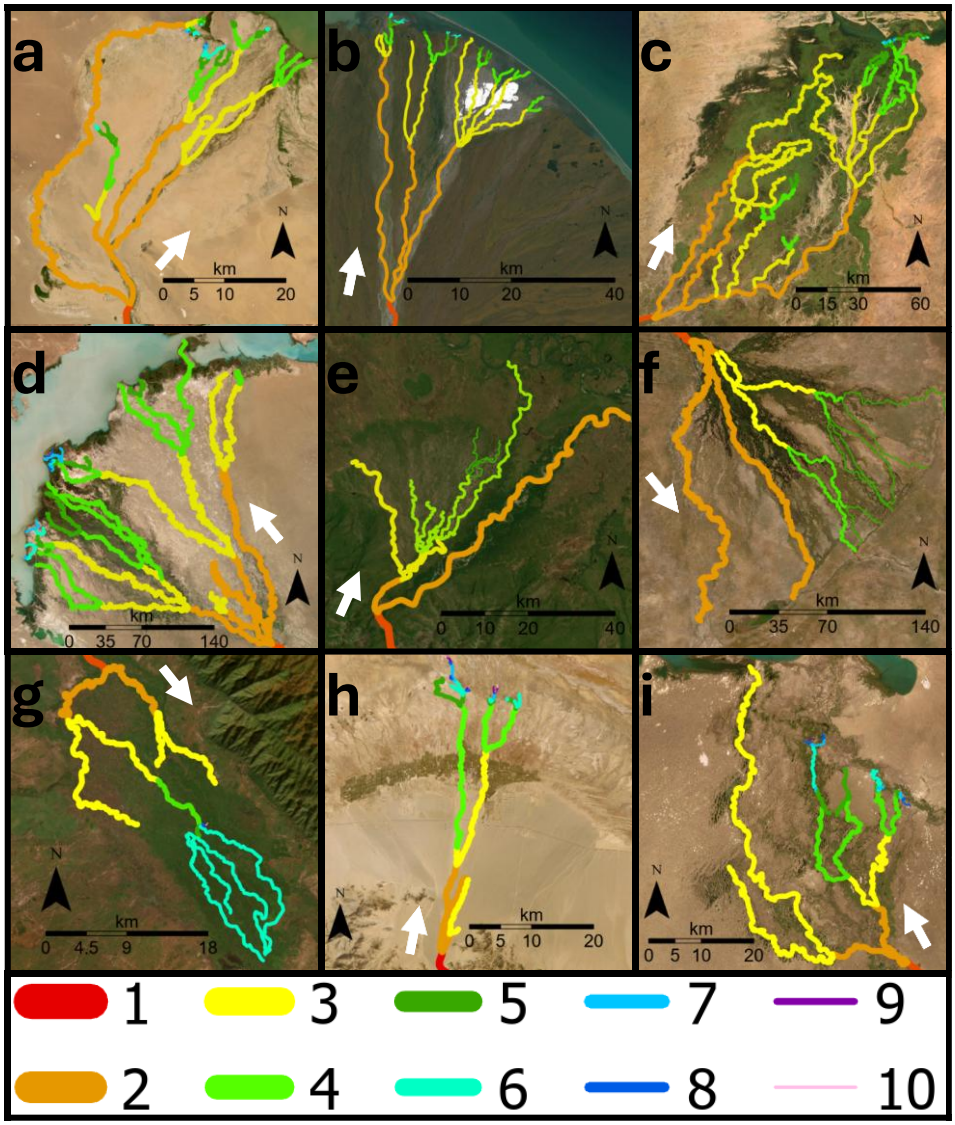

Figure 2: Examples of fluvial fan channel networks: (a) Dzavhan Gol, (b) Kongakut, (c) Niger, (d) Ili, (e) Bayunda, (f) Okavango, (g) Shire, (h) Nomon He, and (i) Aksu fans. The colors indicate channel hierarchy (see Methods), and white arrows indicates downfan direction. Base imagery from Esri's World Imagery basemap (© Esri, DigitalGlobe, GeoEye, i-cubed, USDA FSA, USGS, AEX, Getmapping, Aerogrid, IGN, IGP, swisstopo, and the GIS User Community). Colors and relative line thicknesses indicate channel hierarchy (see Methods), with the widest lines representing order 1 channels and progressively thinner lines representing higher channel orders.

Deleted: Pilcomayo

294

Fluvial fans are distinct landforms from alluvial fans that feature steep gradients (typically 2–12°), have a relatively small radial distance typically less than 10 kilometers, and lack channel networks (Blair & McPherson, 1994; Moscariello, 2018). Although surface channels may occur on alluvial fans, these are transient features formed by surface erosion, and do not construct alluvial fans, which form by a combination of gravitational and sheet flood processes (Blair & McPherson, 1994; Moscariello, 2018). Thus, alluvial fans are not considered here as they are distinct from fluvial fan channel networks that form by river avulsions.

2.3 Morphometric Criteria for Recognition of Delta and Fluvial Fan Channel Networks

Based on the above differences in delta and fluvial fan morphodynamics, we hypothesize that the morphometric differences in their channel networks can be quantified. Based on prior work, we expect river-dominated delta channel networks to display downstream decreasing channel widths and lengths with increasing bifurcation order (Edmonds & Slingerland, 2007; Seybold et al., 2007; Wolinsky et al., 2010), and have an average channel network angle of approximately 72° (Coffey & Shaw, 2017). These metrics should differ in fluvial fans, because the channel networks are built by river avulsions rather than mouth-bar-driven bifurcations. However, delta networks also experience (lobe-scale) avulsions, and we expect some overlap in the network angles. Below, we test these morphometric criteria on 40 river-dominated delta and 40 fluvial fan channel networks (Fig. 3).

3. Dataset and Methods

Although automated channel mapping tools like ChannelExtractor in TopoToolbox (Schwanghart & Kuhn, 2010) and Rivamap (Isikdogan et al., 2017) exist, these methods rely on either terrain-based flow

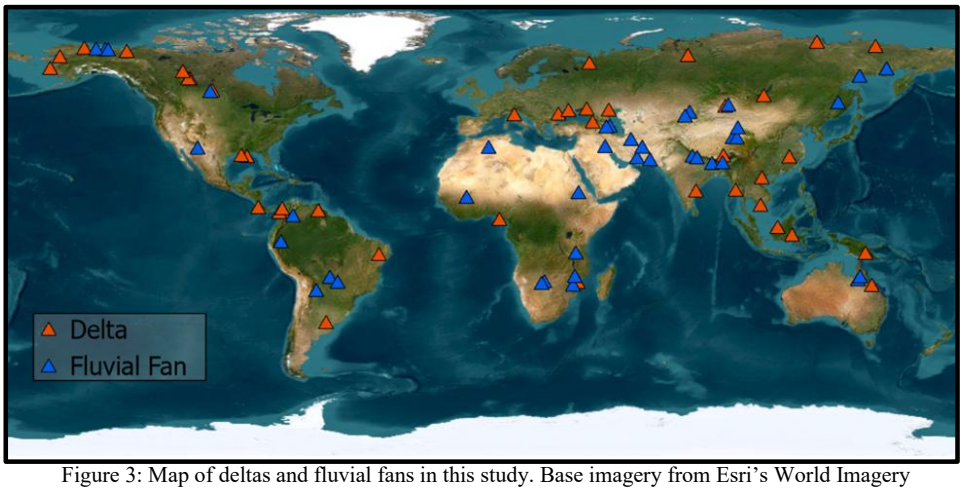

Figure 3: Map of deltas and fluvial fans in this study. Base imagery from Esri's World Imagery basemap (© Esri, DigitalGlobe, GeoEye, i-cubed, USDA FSA, USGS, AEX, Getmapping, Aerogrid, IGN, IGP, swisstopo, and the GIS User Community).

routing or the detection of active surface water, typically based on spectral characteristics, to delineate river channels. However, fluvial fan channel networks are predominantly composed of paleo-channels that lack both clear topographic expression and surface water signatures. Both delta and fluvial fan channels can also be only a few meters wide, often falling below the spatial resolution of commonly available DEMs and remote sensing imagery. In such settings, the coarse resolution and smoothing of subtle terrain in DEMs, especially in low-relief environments, further limit the effectiveness of automated extraction. As a result, we are constrained to manual digitization, as described below.

3.1 Channel Order

To establish channel order in networks, we follow (Dong et al., 2016). Their method follows a simple rule: bifurcations produce downstream increasing channel order through channels that branch. To be considered a channel of a higher order, the resultant channels must not merge downstream. When a first-order channel bifurcates, two second-order channels develop downstream of this bifurcation. When these two channels subsequently bifurcate, two new pairs of third-order channels form, and so on (Figs. 4a and 4b). All channels from the first instance of branching up to and include those that enter a body of water or terminate on land are measured. Identification of bifurcation nodes follows Edmonds et al., (2011), such that the first-order bifurcation for a river channel is the first bifurcation that the channel undergoes (Fig. 4a). Although these methods were developed for deltaic channel networks, here we adapt them for fluvial fan networks also (Figs. 4c and 4d). We do not map or measure channels that loop or rejoin downstream, or channels of non-fluvial origin, such as tidal channels or inlets (Smart, 1971; Tejedor et al., 2015) that are not connected to the fluvial distributary channels. We also omit local avulsions on fluvial fans, which generate channels that typically merge downfan (Slingerland & Smith, 2004). Paleo-channels on fluvial fans were recorded where possible. Paleo-channels resembled active channels that exhibit little to no discharge when we mapped the channel networks (Fig. 4d). We included paleo-channel measurements in fluvial fans because they are ubiquitous in fluvial fans (Hartley et al., 2010), and many of these channels do carry discharge if reactivated during major flood events.

3.2 Channel Length and Width Measurements

Channel length and width measurements follow Edmonds & Slingerland (2007), where channel length is measured as the distance between two bifurcation nodes in deltas (Fig. 4a). We adopt this methodology also to fluvial fans to measure channel lengths between avulsion nodes (Fig. 4c). The average width of a channel segment is recorded from three separate width measurements: one immediately after a node (w_i), one immediately before the next node (w_f), and one halfway between these two points at the midpoint of the channel segment (w_h) (Figs. 4a and 4c). Land–water boundaries in both deltas and fluvial fans were identified visually based on color (with water appearing darker and bluer than land), surface texture, and vegetation contrast. In deltas, channel width measurements were recorded

Deleted: .

Deleted: .

based on the width of water present in the channel, which was nearly always delineated by clear vegetation (Fig. 4b). For channels on fluvial fans, including paleo-channels, bankfull widths were measured from clearly identifiable channel banks, vegetation patterns, and subtle depressions, allowing

Deleted: as observed in the satellite imagery

Deleted: .

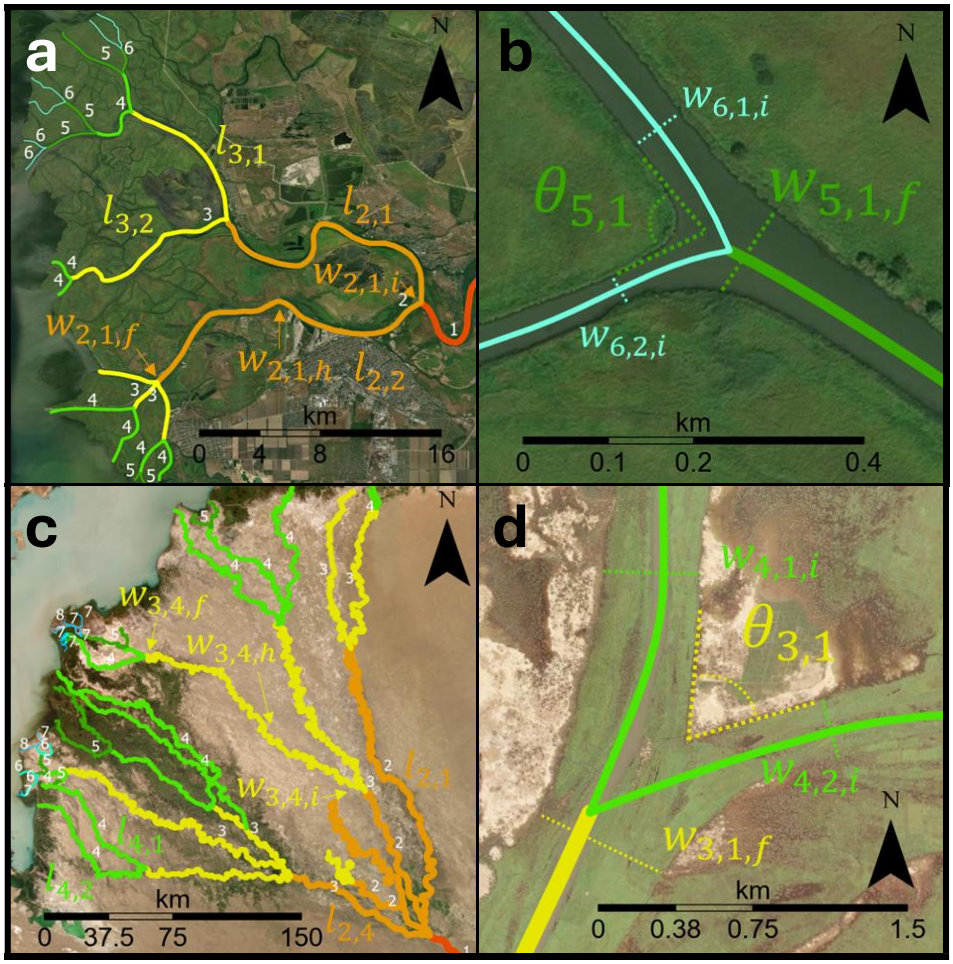

Figure 4: Illustration of (a) channel order, length, and width and (b) bifurcation angle measurements in deltas (Don delta). Illustration of (c) channel order, length, and width (Ili fan) and (d) divergence/crossover angle measurement (Niger fan). Arrows point to locations of w_i = initial channel width, w_h = midpoint channel width, w_f = final width measurements. The w_f is set as the length of two limbs that track along the edges of the mouth bar. θ_n corresponds to the bifurcation or divergence/crossover order. Base imagery from Esri's World Imagery basemap (© Esri, DigitalGlobe, GeoEye, i-cubed, USDA FSA, USGS, AEX, Getmapping, Aerogrid, IGN, IGP, swisstopo, and the GIS User Community).

for the mapping of dry or inactive channels (Fig. 4d). These approaches allowed measurement of inactive channels while maintaining a uniform methodology and consistency for all width measurements. The smallest measured channel widths resolvable in the imagery were 2-meters for deltas and 1-meters for fluvial fans. Width measurements were not performed in locations where a channel has locally split into multiple branches that join downstream.

Given the maximum 0.5-meter spatial resolution of the imagery (see Methods section 3.5), measuring channels only a few meters wide carries some uncertainty. Normalization to the first-order channel width helps mitigate this effect and reduce variability across systems. All channel width measurements were normalized using the initial first-order channel width, following the methodology of Edmonds & Slingerland, (2007). Consequently, the normalized channel width value for first-order channels is always equal to one. First-order channel lengths were measured between the last occurrence of tributary channels and the first channel splitting node and contain no significant value for our study. Moreover, manual digitization of fluvial fan channels spanning tens of kilometers may introduce minor inconsistencies in channel path representation, particularly for narrow (<10 m) and highly sinuous channels. All channel length measurements (l) were also normalized using the first order channel width measurements according to existing methodologies (Edmonds & Slingerland, 2007; Jerolmack, 2009), and this too helped to reduce uncertainties when digitizing channel lengths. As such, the normalized first order channel length values merely reflect our selected methodologies rather than an attributable morphological characteristic.

3.3 Network Angle Measurements

To quantify network angles, we adopt the methodology of Coffey & Shaw, (2017) developed for measuring channel bifurcation angles, which determines the angles of mouth bars formed at the end of an upstream channel. In this methodology, the final channel width directly upstream of a bifurcation (w_f) is set as the length for two limbs of an angle that follows the mouth bar-water contact to measure a bifurcation angle (θ_n) (Coffey & Shaw, 2017) (Fig. 4b). The same methodology is adapted here for fluvial fans (Fig. 4d). In some river deltas, tidal processes cause bifurcation of a channel into three channels instead of two; these are referred to as trifurcations (Leonardi et al., 2013), furcation (Shaw et al., 2018) or polyfurcations (Chamberlain et al., 2018), and a few such measurements are included in the dataset in the very distal portions of deltas where tidal influence is significant. We do not measure angles where channels loop or rejoin downstream of avulsions or bifurcations. In essence, we focus on the morphology of branching channel networks and measure the visible angles between channels or paleo-channels independent of their origin (Fig. 4b and 4d).

3.4 Global Delta and Fluvial Fan Channel Network Database

Deleted: Channel w

Deleted: eter

Moved up [1]: . In deltas, channel width measurements were recorded based on the width of water present in the channel, as observed in the satellite imagery.

Deleted: For fluvial fans, paleo-channel width measurements were based on the bankfull width, defined by clearly visible channel banks or vegetation boundaries.

Deleted: .

Deleted: reflects

To test the applicability of the proposed criteria, we selected 40 river-dominated deltas and 40 fluvial fans (Fig. 3 and Supplementary Data) to be mapped using composite satellite data (ESRI, 2025). These landforms were selected from a diverse range of hydroclimatic, topographic, and basinal conditions from across the world (Fig. 3).

All deltas have been identified as such by prior work (Broaddus et al., 2022; Galloway, 1975; Hartley et al., 2010; Leier et al., 2005; Nienhuis et al., 2015, 2018; Vulis et al., 2023), and they display active discharge based on satellite imagery. Only river-dominated deltas are included in the dataset, because wave-and tide-dominated delta morphology is distinct from that of fluvial fans. The river dominance of deltas and the presence of tide- or wave-influence was determined using the established principles of process-based delta classification (Broaddus et al., 2022; Galloway, 1975; Nienhuis et al., 2015, 2018; Paniagua-Arroyave and Nienhuis 2024; Vulis et al., 2023). However, categorical discrepancies exist between these different classification approaches. To clarify our terminology, we define "dominated" versus "influenced" deltas as follows. Wave-dominated deltas (e.g. São Francisco, Eel) are characterized by strandplanes and a complete absence of bifurcations; these deltas are excluded from our study. Wave-influenced deltas still possess morphological features such as strandplains, but exhibit clear, measurable channel bifurcations and are included in our study. Similarly, tide-dominated deltas (e.g. Fly, Yangtze) have a limited number of channels that widen substantially seaward, whereas tide-influenced deltas such as the Yukon (Fig. 1c) exhibit channel widening only in the most distal channels (Xu & Plink-Björklund, 2023). In practice, we combine these parameters with established classifications (Broaddus et al., 2022; Galloway, 1975; Nienhuis et al., 2015, 2018; Paniagua-Arroyave & Nienhuis, 2024; Vulis et al., 2023) to categorize the deltas in our study. Please refer to the Supplementary Data for information regarding our classification of each delta. We test the effects of tide- and wave-influence on the morphometric criteria by comparative analyses.

Fluvial fans were located using their apex coordinates from the global fluvial fan database of Hartley et al. (2010). This database also includes data on fluvial fan length, gradient, termination style (axial, contributory, lacustrine, marine, playa, desert/dune, and wetland). Termination styles refer to the environment where the fluvial fan terminates: for instance, a contributory-termination style denotes that the landform channels switch from distributary to contributory at the toe of the fan, while axial fans are classified when the main channel forms a confluence with an axial fluvial system (Hartley et al., 2010). Fluvial fans that enter oceans or lakes were originally distinguished from deltas based on (1) displaying no significant modification of the planform by marine processes, such as wave or tidal influence; or (2) the fluvial fans apex is close to the tidal limit (Hartley et al., 2010). They identified that on relatively high-gradient systems (with slopes above 0.143°) marine reworking is normally restricted to the toe of the fluvial fans and can be easily identified. On relatively low-gradient systems (with slopes below 0.0573°)

Deleted: All deltas have been identified as such by prior work (Broaddus et al., 2022; Galloway, 1975; Hartley et al., 2010; Leier et al., 2005; Nienhuis et al., 2015, 2018; Vulis et al., 2023), and display active discharge based on satellite imagery. ¶

Deleted: ,

Deleted: e.g.

Deleted: The

Deleted: f

Deleted: on the basis of

Deleted: or

Deleted: DFS

Deleted: position

Deleted: (Hartley et al., 2010)

Deleted: 0.0025 or

Deleted: DFS

Deleted: 0.001 or

the influence of marine processes was more difficult to determine, and unless the landform apex was located a significant distance inland (>200 km) the landform was excluded from their database. We added a visual inspection that the channel network is a paleo-channel network, and we test the robustness of the classification by comparative analyses of fluvial fans with lake and ocean terminations vs terrestrial terminations. To further test the robustness of our methodology, we analyze whether the landform size, gradient, termination style, or wave- and tide-influence in deltas affect the results.

3.5 Mapping with ArcGIS Pro

Delta and fluvial fan channel networks were mapped using ArcGIS Pro software (Version 3.2.1) (Fig. 1, 2, and 4) with the ESRI World Imagery basemap, which provides up to 0.5-meter imagery for most of the world (ESRI, 2025). This resolution is suitable for mapping very narrow channels only several meters wide. Alternative datasets such as Landsat (30-meter resolution) or Sentinel-2 (10-meter resolution) are too coarse for this application; however they do contain multispectral bands that could be very useful in defining land-water contacts in places where it is ambiguous for wider channels. While ESRI World Imagery is compiled from multiple providers and acquisition times, producing mosaicked tiles, we did not observe noticeable changes in channel appearance across tile boundaries (e.g., abrupt changes in channel width or discharge).

Another limitation of our dataset is uncertainty regarding the timing of satellite image acquisition relative to precipitation events. Precipitation increases discharge, thereby increasing measured channel widths, particularly for fluvial fans in arid environments. Such events can also reactivate partial avulsions and crevasses, which can potentially increase the apparent number of channels. However, none of the selected systems exhibited observable seasonal or large-scale discharge changes across their channel networks attributable to different timings in data collection. Additionally, because this study relies on values normalized to the initial channel width, the effects of seasonal variability on channel width measurements are minimized.

Two feature classes were created: one for deltas and one for fluvial fans. Each delta or fluvial fan landform was then individually mapped as a shapefile layer under the corresponding feature class (Supplementary Data). The shapefiles for channel networks were created as polyline features, which allow users to manually trace individual river channel segments while automatically recording line lengths. Channel widths and angles were measured using the line and angle measurement tools in ArcGIS Pro. All data was recorded in the attribute table for each landform. This data was organized into Excel documents and subsequently converted to Python- and Pandas- readable CSV files (Supplementary Data).

3.6 Code and Statistics

Kolmogorov-Smirnov and Shapiro-Wilk tests were first applied to determine whether the data are normally distributed. Levene's test was used to test differences in variances of populations that do not

Deleted:

Deleted: ¶
We

Deleted: We also subdivided delta termination styles in lakes and oceans.

Deleted: One

Deleted: methodology

Deleted: channel

Moved up [2]: One limitation of our methodology is uncertainty regarding the timing of satellite image acquisition relative to precipitation events. Precipitation increases channel discharge, thereby increasing measured channel widths, particularly for fluvial fans in arid environments. Such events can also reactivate partial avulsions and crevasses, which can potentially increase the apparent number of channels. However, none of the selected systems exhibited observable seasonal or large-scale discharge changes across their channel networks attributable to different timings in data collection. Additionally, because this study relies on values normalized to the initial channel width, the effects of seasonal variability on channel width measurements are minimized.¶

exhibit a normal distribution (Trauth, 2006). Independent samples or Welch's t-test were then applied to test for a difference in means for populations with similar and dissimilar variances, respectively, while one-sample t-tests were used to test comparisons of a subgroup against the overall population mean (Trauth, 2006). For this study, a p-value less than 0.05 (5% significance level) suggests that the two population distributions, variances, or means are not similar. Data confidence intervals were calculated according to Mendenhall et al., (2012). Data analysis and visualization were performed using Python. Open-source data visualization libraries Matplotlib (Hunter, 2007), NumPy (Harris et al., 2020), SciPy (Virtanen et al., 2020), and Seaborn (Waskom, 2021) were utilized.

4. Results

4.1 Delta and Fluvial Fan Channel Network Angles

The mean channel network angle (θ_d) in deltas is 74.0° with a 95th percentile confidence interval of ± 1.9° (n = 527) (Fig. 5a). The mean channel network angle (θ_f) in fluvial fans is 55.0° ± 2.0° (n = 520) (Fig. 5b). The delta and fluvial fan network angle populations are not normally distributed according to both Kolmogorov-Smirnov (KS) and Shapiro-Wilk (SW) tests, with p-values less than 0.05. Levene's test for statistical difference in variances also results in a p-value less than 0.05, suggesting population variances are statistically different. A subsequent independent sample t-test suggests the means of delta and fluvial fan angle populations are statistically different, with a p-value less than 0.05. All statistical results are recorded in Supplementary Table 1 in the Supplementary Information.

We also reviewed the mean network angle of each individual delta and fluvial fan ($\theta_{Landform}$) (Figs. 5c and 5d), and these analyses reveal some overlap. All fluvial fans have mean angle values less than 60°, except for six landforms, or 15% of fluvial fans in this study. Four of these landforms have mean angles larger than 60° (60.8°, 63.2°, 67.7°, 67.9°), and two larger than the delta mean of 73.7° (79.6°, 80.1°). All individual deltas have mean network angles larger than 60°, except for one delta (59.3°). There are also three deltas with mean angles around 60° (61.5°, 62.4°, 63.3°).

Deleted: 3

Deleted: 8

Deleted: 8

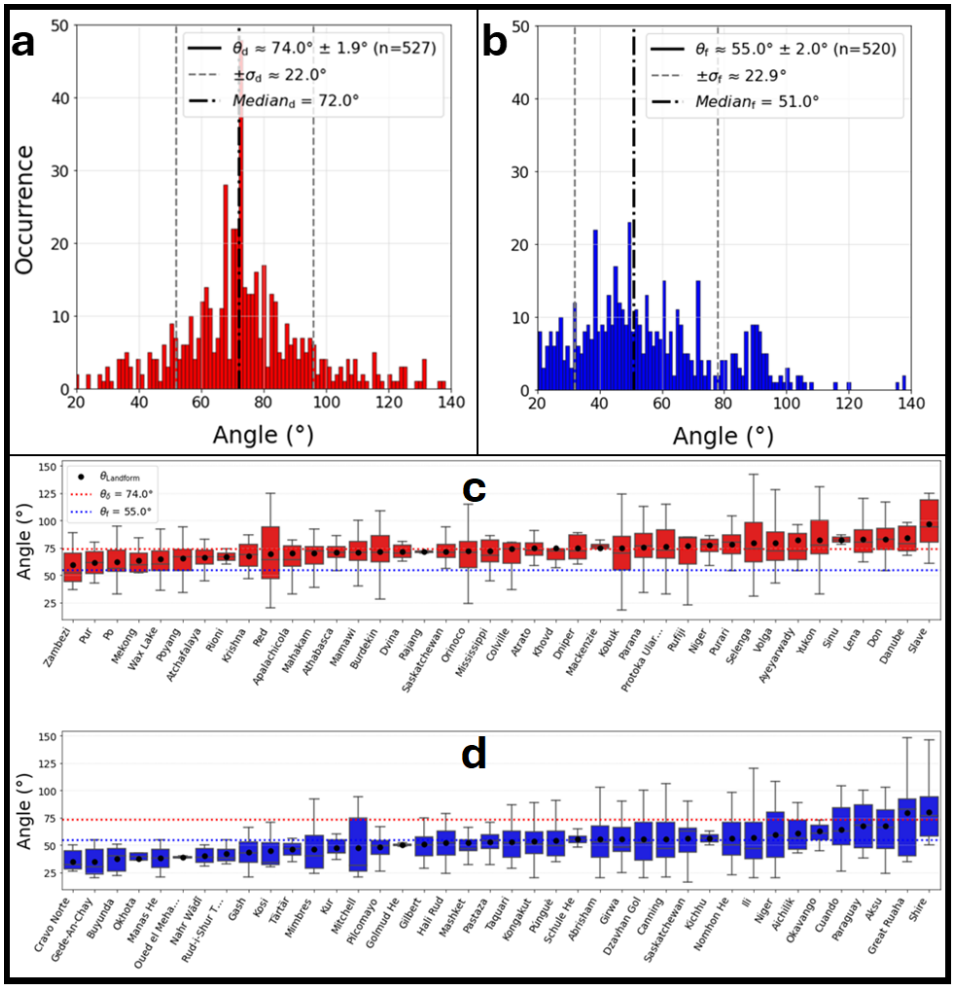

Figure 5: Histograms depicting distributions of (a) delta channel network angles with mean angle (θ_d), its standard deviation (σ_d) and median, and (b) fluvial fan channel network angles with mean fan angle (θ_f), its standard deviation (σ_f)and median. Box-and-whisker plots with the mean angle for each delta (c) and fluvial fan (d) landform ($\theta_{Landform}$).

Deleted: delta

Deleted: ,

Deleted: displayed

Deleted: displaying

The distribution of delta angles grouped by order (Fig. 6a) yields no strong trends for mean angle in deltas. Seventh and tenth order channels have slightly lower mean angle values at 65° and 67°, but these higher-order groups have low sample sizes (n = 3; n = 8) (Fig. 6a). The distribution of fluvial fan angles grouped by order does yield a trend: the mean angle for first- through third-order channels (θ_1, θ_2, and θ_3 in Fig. 6b) is between 47 – 50° and increases to 61 – 63° for fourth- through eight-order channels, and to

66° for ninth-order angles (n = 6) ($\theta_4 - \theta_9$ in Fig. 6b). In contrast to the unimodal distribution of delta angles, the distribution of higher-order fluvial fan angles is bimodal, with a dominant peak near 50° and a secondary peak around 80 – 100° (Fig. 6b).

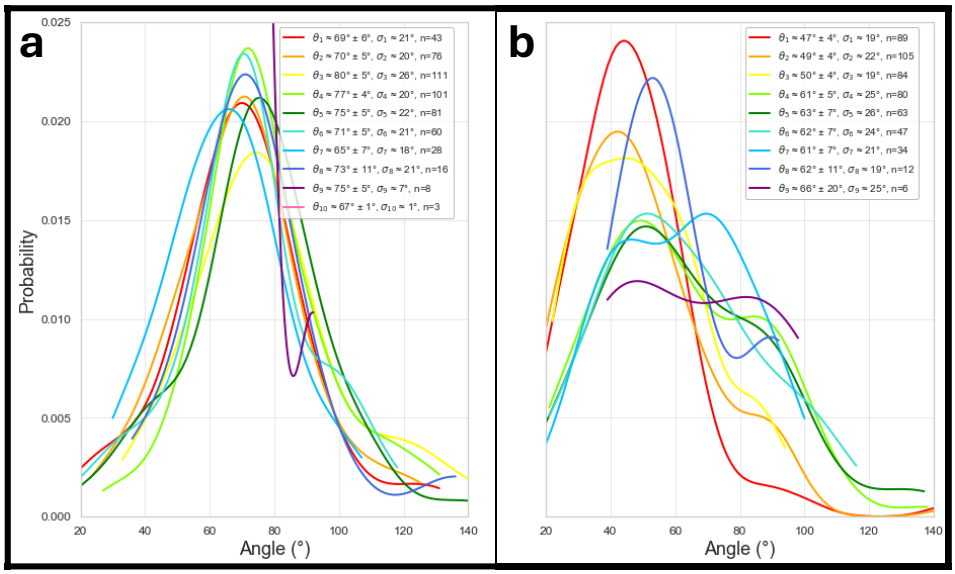

Figure 6: Distribution of (a) delta, and (b) fluvial fan network angles grouped by order (θ_n) with the 95th percent confidence interval. (σ_n) = denotes standard deviation. n denotes sample size.

All deltas in this analysis are river-dominated deltas, however some are tide- or wave-influenced (See Section 3.4 and Supplementary Data). Grouping deltas by process regime shows that the mean network angle for the 19 river-dominated deltas (θ_R = 73.6° ± 2.2°, n = 374), for the 16 tide-influenced deltas (θ_t = 75.6° ± 3.9°, n = 139), and for the 5 wave-influenced deltas (θ_w = 67.1° ± 10.1°, n = 14) (Fig. 7a). The river-dominated and tide-influenced delta angle means are not statistically different from the mean angle for the whole delta population (Supplementary Table 1). The wave-influenced delta angles were omitted from this statistical analysis due to a small sample size (n = 14 < 30).

Many delta angle measurements in this dataset come from Arctic deltas. The comparison between Arctic and non-Arctic deltas shows that Arctic deltas have a larger mean angle (θ_A = 76.5° ± 2.7°, n = 263) than non-Arctic deltas (θ_{NA} = 71.4° ± 2.6°, n = 264) (Fig. 7b). There is a statistically significant difference in means between Arctic and non-Arctic deltas (Supplementary Table 1). Grouping deltas by termination style (Fig. 7c) shows that lake-terminating deltas have slightly smaller mean angles than those that terminate in oceans (θ_L = 72.9° ± 3.2°, n = 160 versus θ_O = 74.4° ± 2.3°, n = 367), but these

Deleted: bifurcation angles
Deleted: divergence/crossover
Deleted: bifurcation
Deleted: 4
Deleted: 5
Deleted: 2
Deleted: 4
Deleted: 5
Deleted: 1
Deleted: 1

differences are not statistically significant compared to the whole delta population (Supplementary Table 1).

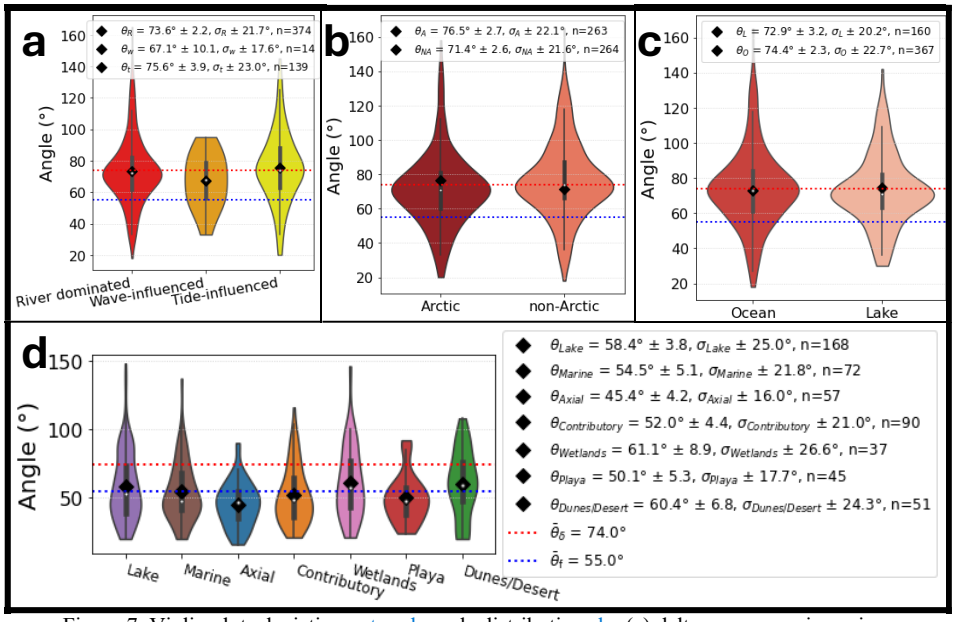

Figure 7: Violin plots depicting network angle distributions by (a) delta process regime: river dominated (θ_R), wave-influenced (θ_w), and tide-influenced (θ_t), (b) deltas in non-Arctic (θ_{NA}) and Arctic (θ_A) climates, (c) ocean terminating deltas (θ_O) and lake terminating deltas (θ_L), and (d) fluvial fan termination styles. All mean angle values have a corresponding 95th percent confidence intervales, standard deviation (σ), and sample count (n).

Deleted: for

Deleted: terminated

Grouping fluvial fans by their termination style shows some differences (Fig. 7d), where the mean angles vary from a low of θ_{Axial} = 45.4° ± 4.2° (n = 57) for axial-terminating fluvial fans to $\theta_{wetlands}$ = 61.1° ± 8.9° (n = 37) for wetland-terminating fans (Fig. 7d). All fluvial fan termination types, except for axial-terminating fans, exhibit population means that are statistically similar to the overall fluvial fan population (Supplementary Table 1). However, each termination style is represented by only 4 to 6 landforms, limiting the statistical power of comparisons and generalizations, despite the relatively robust measurement numbers in wetland (n = 37), playa (n = 45), dunes/desert (n = 51), and axial-terminating fans (n = 57). There also appears to be some discrepancies in Hartley et al., (2010)'s assignment of termination types, such as referring to playa fans as lacustrine or ocean fans as contributory. We also tested whether landform size (Supplementary Fig. 1) and gradient (Supplementary Fig. 2) affect the channel network angles, and these analyses yield no trends, supporting the robustness of our methodology.

4.2 Channel Lengths and Widths

Normalized channel length and width measurements reveal morphological differences between fluvial fan and delta channels. Both landform types show non-linear decreases in these values with increasing channel order (Fig. 8). Statistical analyses confirm that the overall means for normalized channel length and width differ significantly between fluvial fans and deltas (Supplementary Table 1). Fluvial fan channels are generally an order of magnitude longer than delta channels, with a mean normalized length of 147.09 compared to 17.18 for deltas (Figs. 8a and 8c). In contrast, delta channels tend to be slightly wider, with a mean normalized width of 0.40 compared to 0.26 for fluvial fans (Figs. 8b and 8d).

Comparing the normalized dimensions by channel order (Fig. 9) reveals additional trends. The normalized channel widths of lower-order fluvial fan channels (orders 1–5) are significantly longer, and the channel shortening rate is higher compared to deltas (Fig. 9a). The normalized lengths become very similar in orders 7–8, then diverge again for the higher orders where the fluvial fan channel lengths are somewhat longer, but the channel shortening rates are higher in deltas. Normalized channel widths show significant differences for orders 2–8, but not for 9–11. Only a few landforms have channels with orders exceeding 9. Fluvial fan narrowing rates are very high from order 1 and 2, and very low in orders 7–10 (Fig. 9b). The narrowing rates are more uniform in deltas. When comparing individual deltas by process regime, both tide- and wave-influenced deltas have significantly higher mean normalized channel widths relative to the overall delta population (Supplementary Fig. 3 and Supplementary Table 1).

Comparison by fluvial fan termination styles shows that axial- and playa-terminating fans exhibit longer mean normalized channel lengths compared to the whole fluvial fan population, whereas dunes/desert-, marine-, and wetland-terminating fans have shorter mean lengths (Supplementary Fig. 3 and Supplementary Table 1). Contributory- and lake-terminating fans do not differ significantly from the overall mean. Regarding normalized channel widths, axial- and marine-terminating fans have wider channels, while dunes/desert-terminating fans are narrower. Normalized width values for contributory-, lake-, playa-, and wetland-terminating fan channels show no difference from the overall population mean (Supplementary Fig. 3 and Supplementary Table 1). Statistical analyses of channel length and width were not conducted for different fluvial fan termination styles due to insufficient sample sizes ($n < 30$) in most categories.

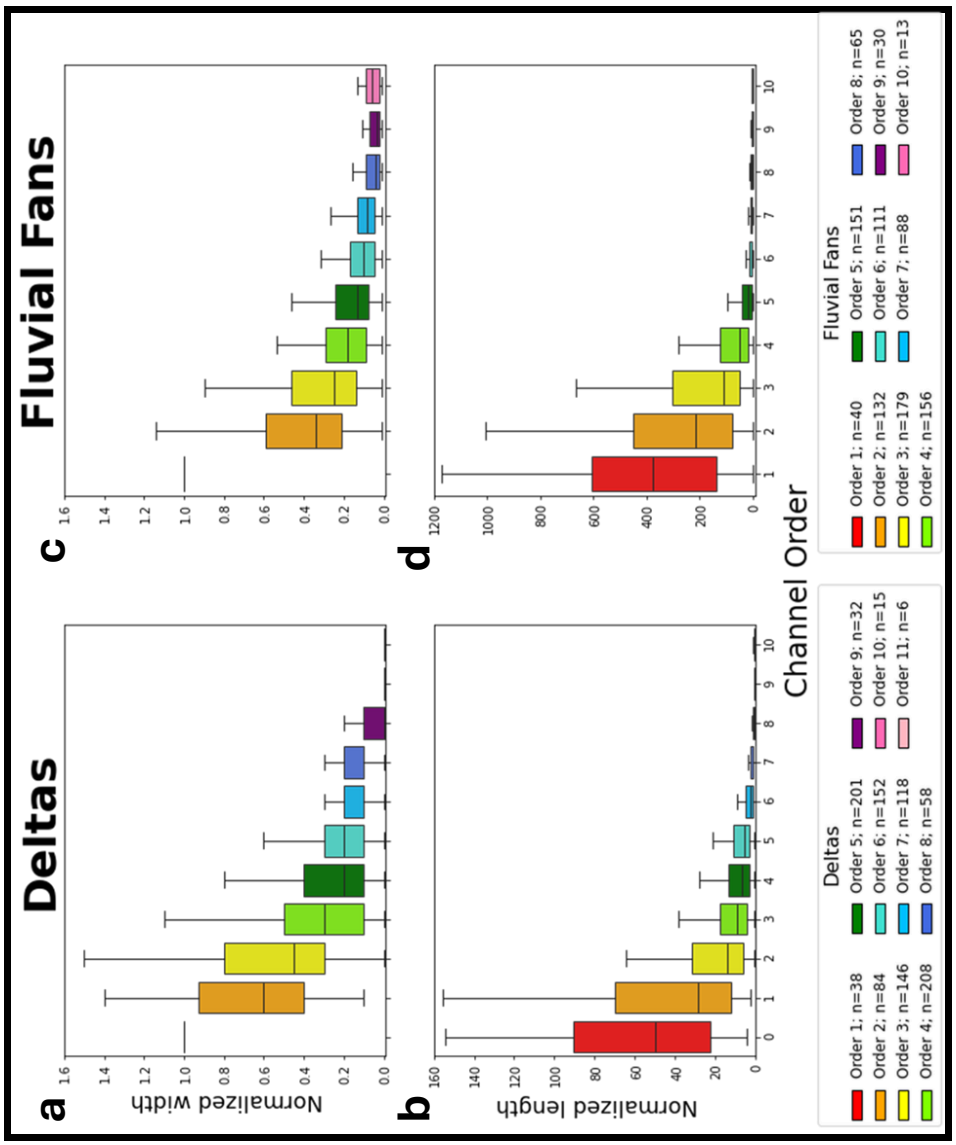

606 Figure 8: Box and whisker plots illustrating normalized delta channel widths (a) and lengths (b), and
607 normalized fluvial fan channel widths (c) and length (d), plotted by channel order. Note the significant difference in normalized channel length scales for subplots b and d.

Deleted: o

Deleted: z

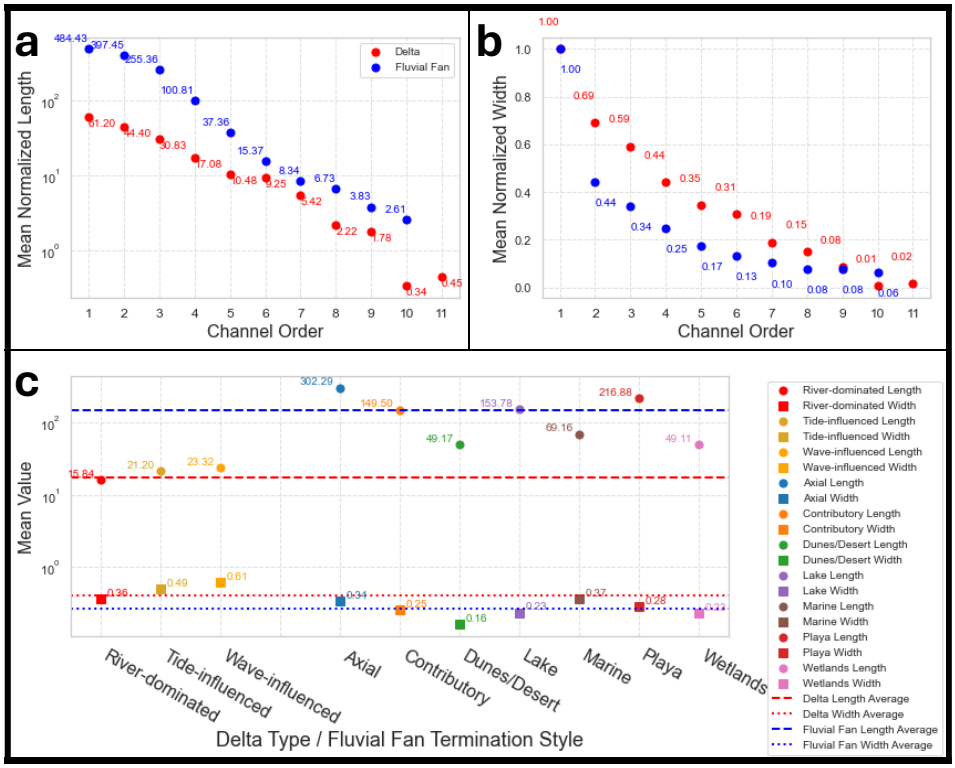

Figure 9: Mean normalized delta and fluvial fan channel (a) length and (b) width values by order. (c) Mean channel length and width values for different types of deltas and fluvial fan termination styles.

Deleted: s by order

5. Discussion

5.1 Effectiveness of Morphometric Criteria in Distinguishing Deltas and Fluvial Fans

The mean channel network angles are distinctly different in deltas and fluvial fans by 20°, and this statistically significant difference is a useful criterion in distinguishing these two landform types. While some overlaps exist at the landform level, these cases are relatively limited, where 15% of fluvial fans in this dataset have a mean angle larger than 60° (Fig. 5d) and 10% of deltas have a mean angle less than 64° (Fig. 5c). These findings support the utility of mean branching angles as a distinguishing metric between deltas and fluvial fans. However, some degree of uncertainty remains, and additional criteria are necessary for more robust distinction.

An additional criterion is the distribution of mean angles by channel order, where fluvial fans have increased mean angles and a bimodal distribution in orders 4–8 (Fig. 6). Other supportive criteria may be

the differences in values and distributions of the normalized channel lengths and widths (Figs. 8 and 9), but the low sample numbers do not allow us to test these criteria by individual landforms. A useful criterion would be to link channel narrowing with the bifurcation and avulsion nodes. In deltas, the downstream channel narrowing occurs in a stepwise manner at the mouth-bar-driven bifurcation nodes, whereas in fluvial fans this decrease should be gradual and not linked to the node positions where full avulsions occur. Our data was collected in a manner that does not permit these analyses.

A potential source of overlap in the delta and fluvial fan channel network mean angles is that not all measured angles in deltas are mouth-bar-driven bifurcation angles, as deltas also experience avulsions (e.g., Fig. 1e). A closer inspection of the four deltas with low mean network angles reveals that each contains very few measurements (n = 3, n = 4, n = 6, n = 7). In these cases, the limited sample size allows the rarer avulsion angles to affect the mean values more strongly. Also, fluvial fans that terminate in a lake or ocean may have terminal channels that form due to mouth bar deposition and channel bifurcation. However, we do not believe these instances affect our results since we do not see that lake- or marine-terminating fans exhibit higher mean angles (Fig. 7d).

Examining fluvial fans with high mean angles shows that these are low-gradient wetland fans, where the avulsion angles tend to be wider as a function of avulsion mechanisms (see Discussion below). However, they may also suggest methodological limitations. While the local avulsion angles in low-gradient wetland fans are wide (measured the final channel width directly upstream of a branching node (w_f) as the length for two limbs of an angle; Fig. 4), angles between the longer channel reaches are considerably narrower (Supplementary Fig. 4). This channel reach angle discrepancy is consistent with similar channel reach angle measurements from (Coffey & Shaw, 2017). We plan to further develop angle measurement methods to capture both the local and the reach-scale angles in future work. It is also important to discuss the limitations of the applied methodologies in the context of the results. Our channel network methodologies are designed for delta channel networks, and exclude channels that merge downstream, which can exclude many potential measurements from fluvial fans in situations where their channels merge downfan.

Deleted: bifurcation

In summary, this initial attempt to distinguish deltas and fluvial fans demonstrates that quantifying channel network angles, and trends in normalized channel widths and lengths provide efficient criteria. However, we also show that sample sizes are important for accurate recognition of landforms, and collecting a sufficient number of angle measurements ($n \gtrapprox 10$) can help account for the infrequent avulsion in deltas or bifurcation in fluvial fans. While each metric is informative on its own, the combination of branching angles, branching angle trends, and normalized channel lengths provides the clearest distinction between deltas and fluvial fans.

5.2 Processes that determine delta and fluvial fan channel network angles

While the 72° mean mouth-bar-driven bifurcation angle is linked to flow patterns at channel tips well-explained by diffusive processes (Coffey & Shaw, 2017), there is currently no established explanation for the approximately 55° mean network angle in fluvial fans. In deltas, mouth-bar-driven bifurcation is the product of sedimentation from turbulent jets that form at the mouths of rivers entering basins (Bates, 1953; Coffey & Shaw, 2017; Edmonds & Slingerland, 2007; Fagherazzi et al., 2015; Jerolmack & Swenson, 2007; Wright, 1977). Once a mouth bar is formed, the flow through the distributary channel bifurcations can be modeled as diffusive flow (Coffey & Shaw, 2017), and the resulting critical angle of 72° represents a stable morphology for the bifurcation as it grows in a diffusive groundwater field (Devauchelle et al., 2012; Ke et al., 2019). The slightly larger network angles in Arctic deltas may reflect environmental influences such as ice cover, permafrost, or limitations on overbank flow (Lauzon et al., 2019; Piliouras et al., 2021; Walker, 1998).

River avulsions are set up by channel superelevation (Mohrig et al., 2000), or when the slope down the flanks of the channel provides a steeper descent than the existing river channel (Slingerland & Smith, 1998; Törnqvist & Bridge, 2002). Avulsions result from channel bed aggradation that reduces the channel capacity (Bryant et al., 1995). Once an avulsion is triggered and full or partial river flow exits the channel, a new channel is generated by surface runoff erosion. Thus, the prevailing topographic gradient would tend to keep the nearby flows more focused in a slope-parallel direction, resulting in narrower network angles compared to mouth-bar-driven bifurcations (Fig. 5b).

The contrast between diffusion-dominated and surface runoff erosion-dominated processes in shaping delta versus fluvial fan channel network topology is further supported by tributary channel network analyses that originally defined the critical angle of 72° (Devauchelle et al., 2012). Tributary channel network analyses show that the mean tributary angle of 72° only occurs in humid catchments with high groundwater recharge, where tributary networks are shaped by groundwater diffusion (Seybold et al., 2017). In contrast, the mean tributary network angle is 45° in arid landscapes where surface runoff dominates (Seybold et al., 2017), or is even lower in the driest catchments (Seybold et al., 2018).

Fluvial fan gradient decreases progressively downstream (e.g. Chakraborty et al., 2010), such that higher gradients near the fan apex likely generate more acute angles, whereas the very low gradients near the toe of the fan would allow for wider angles. This trend likely explains the downstream increase in fluvial fan network angles and the emergence of the second, wider peak in higher order channels (Fig. 6b). Furthermore, avulsion mechanisms have been shown to change from channel superelevation in upstream river reaches, where river gradients are steeper, to gradient advantage in downstream low-gradient reaches (Gearon et al., 2024). In these low-gradient zones, crevassing processes can produce high-angle deviations with the angle values around 90° (Rahman et al., 2022). Avulsion angles above 100° have been measured in meandering rivers on low-gradient floodplains with vegetation (see Rahman

Deleted: can be explained by

Commented [PP4]: There is something wrong with this sentence. I think I fixed it

Deleted: as a process

et al., 2022). These effects may be important controls in the fluvial fan channel networks in low-gradient vegetated wetlands. Reitz & Jerolmack, (2012) show that abandoned paleo-channel reoccupation may control new avulsion positions, and paleo-channel density is highest in the narrower fan apex. Avulsion angles may also change over time due to evolving channel width ratios (Morais & Montanher, 2022), or may be affected by a critical angle or bend curvature (Yang, 2020). Future work targeting how avulsion morphology evolves downfan would provide important insight into the mechanisms driving the observed increase in angles downstream.

We thus conclude that the distinction between deltaic and fluvial fan channel network angles arises from the dominant formative processes: diffusive flow in deltas versus surface runoff erosion in fluvial fans. Furthermore, in fluvial fans, network angles appear to be negatively correlated with surface gradients, with lower gradients allowing for wider avulsion angles.

5.3 Ancient deltas and fluvial fans

Our proposed methodology could also be used to distinguish ancient fluvial fans and deltas, for instance in seismic datasets, where only delta channel network angles have been quantified before (Mahon et al., 2024). Our results confirm the prior modern data (Chakraborty et al., 2010) and recent modeling outcomes (Martin & Edmonds, 2023), and help to eliminate a discrepancy in plan-view versus cross-sectional fluvial fan facies models (Plink-Björklund, 2021). Namely, earlier work suggested processes similar to mouth-bar-driven bifurcations as a key mechanism driving fluvial fan formation (Friend, 1978; Kelly & Olsen, 1993; Weissman et al., 2010), probably due to downstream channel narrowing. However, this hypothesis contradicts the stratigraphic data that indicate that proximal fans consist of amalgamated channel deposits (Chakraborty et al., 2010; Kelly & Olsen, 1993; Nichols & Fisher, 2007; Singh et al., 1993; Weissman et al., 2013) – a pattern consistent with frequent avulsions (Chakraborty et al., 2010; Singh et al., 1993).

Deleted: bifurcations

5.4 Sensitivity of Deltas and Fluvial Fans to Global Change

Deltas and fluvial fans differ significantly in their vulnerability to natural hazards and in their responses to global change. Deltas are highly vulnerable to coastal hazards and sea level rise (Giosan et al., 2014; Syvitski et al., 2009). Rising sea-levels will not only inundate deltaic distributary networks, but also cause a landward migration of the avulsion node corresponding with the landward shift of the backwater zone (Brooke et al., 2022; Chatanantavet et al., 2012; Ganti et al., 2014). This process reduces sediment delivery to shorelines, accelerating the effects of sea-level rise. However, changes in land use and changing precipitation patterns which increase sediment supply could complicate the picture by shifting delta avulsion sites seaward (Brooke et al., 2022). In contrast, fluvial fans are controlled by upstream morphodynamics, where the fan location (apex) is pinned by a steep topographic break (Brooke et al., 2022; Ganti et al., 2014; Martin & Edmonds, 2023). For coastal fans, sea-level rise and coastal

erosion would affect the fan toes, however the avulsion node at the fan apex and sediment deposition across most of the fan surface would not be affected, making fluvial fans significantly less vulnerable to sea-level rise.

Deleted: drowning

Both deltas and fluvial fans are affected by reduced sediment supply due to river damming and artificial levees (Blum & Roberts, 2009; Giosan et al., 2014; Nienhuis et al., 2020; Paola et al., 2011; Syvitski et al., 2009). However, fluvial fans are highly sensitive to the water and sediment supply changes, such as changes in precipitation patterns (Assine et al., 2014; Hansford & Plink-Björklund, 2020; Leier et al., 2005). Increases in extreme precipitation cause a significant increase in avulsion frequency and crevassing splay formation (Morón et al., 2017), because large fluctuations in river discharge, such as during extreme precipitation events, are avulsion-triggering events (Jones & Schumm, 1999). Indeed, fluvial fans have been shown to be highly sensitive to such changes, where fluvial fan activation and deactivation cycles have been linked to millennial-scale changes in monsoon intensity or precipitation patterns (Assine et al., 2014; Fontana et al., 2014, Latrubesse et al., 2012).

6. Conclusions

This study demonstrates that river-dominated delta and fluvial fan channel networks can be distinguished using quantitative morphometric criteria derived from their channel network topology. Deltaic networks are primarily shaped by mouth-bar-driven bifurcation processes, resulting in mean bifurcation angles of approximately 74°, consistent with diffusion-dominated growth. In contrast, fluvial fan topology is shaped by channel avulsions, producing narrower mean network angles near 55°, indicative of surface runoff processes. Fluvial fan network angles tend to widen downstream, likely due to decreasing gradients and avulsion style shifts, while delta angles remain relatively consistent, reflecting persistent mouth-bar-driven bifurcation processes. Both channel networks display downstream reductions in channel length and width with increasing channel order, but the fluvial fan networks are characterized by significantly longer and somewhat narrower channels when normalized.

These differences not only support the use of network morphology as a diagnostic tool for identifying ancient fluvial fans and deltas in the stratigraphic record or other planetary bodies but also provide insights into their differing sensitivities to environmental change.

Code Availability

The Python code used for data analysis and figure generation was created and run in Jupyter Notebook version 6.4.8 (Anaconda distribution).

Data Availability

Morphological data collected in this study are available at https://github.com/lukegezovich/Delta-and-Fluvial-Fan-Networks.

Author Contribution

Luke Gezovich was responsible for the investigation and data curation, development of methodology, formal analysis and visualization, and writing the original draft of the manuscript. Piret Plink-Björklund initiated the project, co-developed the initial methodology, and co-wrote the manuscript. Jack Henry co-developed the initial methodology and perform initial mapping and analyses of a small number of systems.

Deleted: contributed to the conceptualization of the project, assisted in methodology development, and provided extensive input through review and editing, as well as with data analysis

Deleted: contributed to methodology development and validation by mapping deltas and fluvial fans, helping to establish consistent mapping approaches and supporting the overall validity of the concept.

Competing Interests

The authors declare that they have no conflict of interest.

Acknowledgments

We thank Kamini Singha, Lesli Wood, and Wendy Zhou for their constructive feedback that helped improve earlier versions of this manuscript. We also thank John Shaw, Ellen Chamberlin, Anastasia Piliouras, and an anonymous reviewer for their helpful comments on the present versions of the manuscript.

Financial Support

Luke Gezovich thanks the American Association of Petroleum Geologists (AAPG) Foundation John & Erika Lockridge Grant, the American Institute of Professional Geologists (AIPG) William J. Siok Graduate Scholarship, the Colorado Scientific Society (CSS), the Rocky Mountain Association of Geologists (RMAG), and the Society for Sediment Geology (SEPM) for providing funding to support this research.

References

Allen, P. A. (2008). Time scales of tectonic landscapes and their sediment routing systems. *Geological Society, London, Special Publications*, *296*(1), 7–28. https://doi.org/10.1144/SP296.2

Assine, M. L. (2005). River avulsions on the Taquari megafan, Pantanal wetland, Brazil. *Geomorphology*, *70*(3–4), 357–371. https://doi.org/10.1016/j.geomorph.2005.02.013

Assine, M. L., Corradini, F. A., Pupim, F. D. N., & McGlue, M. M. (2014). Channel arrangements and depositional styles in the São Lourenço fluvial megafan, Brazilian Pantanal wetland. *Sedimentary Geology*, *301*, 172–184. https://doi.org/10.1016/j.sedgeo.2013.11.007

Axelsson, V. (1967). The Laitaure Delta: A Study of Deltaic Morphology and Processes. *Geografiska Annaler. Series A, Physical Geography*, *49*(1), 1. https://doi.org/10.2307/520865

Bates, C. C. (1953). Rational Theory of Delta Formation. *AAPG Bulletin*, *37*. https://doi.org/10.1306/5CEADD76-16BB-11D7-8645000102C1865D

Bentley, S. J., Blum, M. D., Maloney, J., Pond, L., & Paulsell, R. (2016). The Mississippi River source-to-sink system: Perspectives on tectonic, climatic, and anthropogenic influences, Miocene to Anthropocene. *Earth-Science Reviews*, *153*, 139–174. https://doi.org/10.1016/j.earscirev.2015.11.001

Blair, T. C., & McPherson, J. G. (1994). Alluvial Fans and their Natural Distinction from Rivers Based on Morphology, Hydraulic Processes, Sedimentary Processes, and Facies Assemblages. *SEPM Journal of Sedimentary Research*, *Vol. 64A*. https://doi.org/10.1306/D4267DDE-2B26-11D7-8648000102C1865D

Blum, M. D., & Roberts, H. H. (2009). Drowning of the Mississippi Delta due to insufficient sediment supply and global sea-level rise. *Nature Geoscience*, *2*(7), 488–491. https://doi.org/10.1038/ngeo553

Bramble, M. S., Goudge, T. A., Milliken, R. E., & Mustard, J. F. (2019). Testing the deltaic origin of fan deposits at Bradbury Crater, Mars. *Icarus*, *319*, 363–366. https://doi.org/10.1016/j.icarus.2018.09.024

Broaddus, C. M., Vulis, L. M., Nienhuis, J. H., Tejedor, A., Brown, J., Foufoula-Georgiou, E., & Edmonds, D. A. (2022). First-Order River Delta Morphology Is Explained by the Sediment Flux Balance From Rivers, Waves, and Tides. *Geophysical Research Letters*, *49*(22). https://doi.org/10.1029/2022GL100355

Brooke, S., Chadwick, A. J., Silvestre, J., Lamb, M. P., Edmonds, D. A., & Ganti, V. (2022). Where rivers jump course. *Science*, *376*(6596), 987–990. https://doi.org/10.1126/science.abm1215

Bryant, M., Falk, P., & Paola, C. (1995). Experimental study of avulsion frequency and rate of deposition. *Geology*, *23*(4), 365. https://doi.org/10.1130/0091-7613(1995)023%253C0365:ESOAFA%253E2.3.CO;2

Chakraborty, T., Kar, R., Ghosh, P., & Basu, S. (2010). Kosi megafan: Historical records, geomorphology and the recent avulsion of the Kosi River. *Quaternary International*, *227*(2), 143–160. https://doi.org/10.1016/j.quaint.2009.12.002

Chamberlain, E. L., Törnqvist, T. E., Shen, Z., Mauz, B., & Wallinga, J. (2018). Anatomy of Mississippi Delta growth and its implications for coastal restoration. *Science Advances*, *4*(4), eaar4740. https://doi.org/10.1126/sciadv.aar4740

Chatanantavet, P., & Lamb, M. P. (2014). Sediment transport and topographic evolution of a coupled river and river plume system: An experimental and numerical study: EXPERIMENTS COUPLED RIVER & RIVER-PLUME. *Journal of Geophysical Research: Earth Surface*, *119*(6), 1263–1282. https://doi.org/10.1002/2013JF002810

Chatanantavet, P., Lamb, M. P., & Nittrouer, J. A. (2012). Backwater controls of avulsion location on deltas. *Geophysical Research Letters*, *39*(1), 2011GL050197. https://doi.org/10.1029/2011GL050197

Chen, C., Tian, B., Schwarz, C., Zhang, C., Guo, L., Xu, F., Zhou, Y., & He, Q. (2021). Quantifying delta channel network changes with Landsat time-series data. *Journal of Hydrology*, *600*, 126688. https://doi.org/10.1016/j.jhydrol.2021.126688

Coffey, T. S., & Shaw, J. B. (2017). Congruent Bifurcation Angles in River Delta and Tributary Channel Networks. *Geophysical Research Letters*, *44*(22). https://doi.org/10.1002/2017GL074873

Davidson, S. K., & Hartley, A. J. (2014). A Quantitative Approach To Linking Drainage Area and Distributive-Fluvial-System Area In Modern and Ancient Endorheic Basins. *Journal of Sedimentary Research*, *84*(11), 1005–1020. https://doi.org/10.2110/jsr.2014.79

Davidson, S. K., Hartley, A. J., Weissmann, G. S., Nichols, G. J., & Scuderi, L. A. (2013). Geomorphic elements on modern distributive fluvial systems. *Geomorphology*, *180–181*, 82–95. https://doi.org/10.1016/j.geomorph.2012.09.008

De Toffoli, B., Plesa, A. -C., Hauber, E., & Breuer, D. (2021). Delta Deposits on Mars: A Global Perspective. *Geophysical Research Letters*, *48*(17), e2021GL094271. https://doi.org/10.1029/2021GL094271

Devauchelle, O., Petroff, A. P., Seybold, H. F., & Rothman, D. H. (2012). Ramification of stream networks. *Proceedings of the National Academy of Sciences*, *109*(51), 20832–20836. https://doi.org/10.1073/pnas.1215218109

Di Achille, G., & Hynek, B. M. (2010). Ancient ocean on Mars supported by global distribution of deltas and valleys. *Nature Geoscience*, *3*(7), 459–463. https://doi.org/10.1038/ngeo891

Dong, T. Y., Nittrouer, J. A., Il'icheva, E., Pavlov, M., McElroy, B., Czapiga, M. J., Ma, H., & Parker, G. (2016). Controls on gravel termination in seven distributary channels of the Selenga River Delta, Baikal Rift basin, Russia. *Geological Society of America Bulletin*, *128*(7–8), 1297–1312. https://doi.org/10.1130/B31427.1

Donselaar, M. E., Cuevas Gozalo, M. C., & Moyano, S. (2013). Avulsion processes at the terminus of low-gradient semi-arid fluvial systems: Lessons from the Río Colorado, Altiplano endorheic basin, Bolivia. *Sedimentary Geology*, *283*, 1–14. https://doi.org/10.1016/j.sedgeo.2012.10.007

Edmonds, D. A., Martin, H. K., Valenza, J. M., Henson, R., Weissmann, G. S., Miltenberger, K., Mans, W., Moore, J. R., Slingerland, R. L., Gibling, M. R., Bryk, A. B., & Hajek, E. A. (2022). Rivers in reverse: Upstream-migrating dechannelization and flooding cause avulsions on fluvial fans. *Geology*, *50*(1), 37–41. https://doi.org/10.1130/G49318.1

Edmonds, D. A., Paola, C., Hoyal, D. C. J. D., & Sheets, B. A. (2011). Quantitative metrics that describe river deltas and their channel networks. *Journal of Geophysical Research*, *116*(F4), F04022. https://doi.org/10.1029/2010JF001955

Edmonds, D. A., & Slingerland, R. L. (2007). Mechanics of river mouth bar formation: Implications for the morphodynamics of delta distributary networks. *Journal of Geophysical Research: Earth Surface*, *112*(F2), 2006JF000574. https://doi.org/10.1029/2006JF000574

ESRI. (2025). *World Imagery* [Imagery layer]. Esri, Maxar. https://www.arcgis.com/home/item.html?id=10df2279f9684e4a9f6a7f08febac2a9

Fagherazzi, S. (2008). Self-organization of tidal deltas. *Proceedings of the National Academy of Sciences*, *105*(48), 18692–18695. https://doi.org/10.1073/pnas.0806668105

Fagherazzi, S., Edmonds, D. A., Nardin, W., Leonardi, N., Canestrelli, A., Falcini, F., Jerolmack, D. J., Mariotti, G., Rowland, J. C., & Slingerland, R. L. (2015). Dynamics of river mouth deposits. *Reviews of Geophysics*, *53*(3), 642–672. https://doi.org/10.1002/2014RG000451

Farley, K. A., Williford, K. H., Stack, K. M., Bhartia, R., Chen, A., De La Torre, M., Hand, K., Goreva, Y., Herd, C. D. K., Hueso, R., Liu, Y., Maki, J. N., Martinez, G., Moeller, R. C., Nelessen, A., Newman, C. E., Nunes, D., Ponce, A., Spanovich, N., … Wiens, R. C. (2020). Mars 2020 Mission Overview. *Space Science Reviews*, *216*(8), 142. https://doi.org/10.1007/s11214-020-00762-y

Federici, B., & Paola, C. (2003). Dynamics of channel bifurcations in noncohesive sediments. *Water Resources Research*, *39*(6), 2002WR001434. https://doi.org/10.1029/2002WR001434

Fielding, C. R., Ashworth, P. J., Best, J. L., Prokocki, E. W., & Smith, G. H. S. (2012). Tributary, distributary and other fluvial patterns: What really represents the norm in the continental rock record? *Sedimentary Geology*, *261–262*, 15–32. https://doi.org/10.1016/j.sedgeo.2012.03.004

Fontana, A., Mozzi, P., & Marchetti, M. (2014). Alluvial fans and megafans along the southern side of the Alps. *Sedimentary Geology*, *301*, 150–171. https://doi.org/10.1016/j.sedgeo.2013.09.003

Friend, P. F. (1978). *DISTINCTIVE FEATURES OF SOME ANCIENT RIVER SYSTEMS*.

Galloway, E. (1975). Process Framework for Describing the Morphologic and Stratigraphic Evolution of Deltaic Depositional Systems. *Deltas: Models for Exploration, 1975*, 87–98.

Ganti, V., Chu, Z., Lamb, M. P., Nittrouer, J. A., & Parker, G. (2014). Testing morphodynamic controls on the location and frequency of river avulsions on fans versus deltas: Huanghe (Yellow River), China. *Geophysical Research Letters*, *41*(22), 7882–7890. https://doi.org/10.1002/2014GL061918

Gearon, J. H., Martin, H. K., DeLisle, C., Barefoot, E. A., Mohrig, D., Paola, C., & Edmonds, D. A. (2024). Rules of river avulsion change downstream. *Nature*, *634*(8032), 91–95. https://doi.org/10.1038/s41586-024-07964-2

Geleynse, N., Storms, J. E. A., Walstra, D.-J. R., Jagers, H. R. A., Wang, Z. B., & Stive, M. J. F. (2011). Controls on river delta formation; insights from numerical modelling. *Earth and Planetary Science Letters*, *302*(1–2), 217–226. https://doi.org/10.1016/j.epsl.2010.12.013

Giosan, L., Syvitski, J., Constantinescu, S., & Day, J. (2014). Climate change: Protect the world's deltas. *Nature*, *516*(7529), 31–33. https://doi.org/10.1038/516031a

Hansford, M. R., & Plink-Björklund, P. (2020). River discharge variability as the link between climate and fluvial fan formation. *Geology*, *48*(10), 952–956. https://doi.org/10.1130/G47471.1

Hariharan, J., Piliouras, A., Schwenk, J., & Passalacqua, P. (2022). Width-Based Discharge Partitioning in Distributary Networks: How Right We Are. *Geophysical Research Letters*, *49*(14), e2022GL097897. https://doi.org/10.1029/2022GL097897

Harris, C. R., Millman, K. J., van der Walt, S. J., Gommers, R., Virtanen, P., Cournapeau, D., Wieser, E., Taylor, J., Berg, S., Smith, N. J., Kern, R., Picus, M., Hoyer, S., van Kerkwijk, M. H., Brett, M., Haldane, A., del Río, J. F., Wiebe, M., Peterson, P., … Oliphant, T. E. (2020). Array programming with NumPy. *Nature*, *585*(7825), 357–362. https://doi.org/10.1038/s41586-020-2649-2

Hartley, A. J., Weissmann, G. S., Nichols, G. J., & Warwick, G. L. (2010). Large Distributive Fluvial Systems: Characteristics, Distribution, and Controls on Development. *Journal of Sedimentary Research*, *80*(2), 167–183. https://doi.org/10.2110/jsr.2010.016

Horton, B. K., & Decelles, P. G. (2001). *Modern and ancient Fluvial megafans in the foreland basin system of the central Andes, southern Bolivia: Implications for drainage network evolution in fold-thrust belts* (pp. 43–63).

Hunter, J. D. (2007). MATPLOTLIB - 2D GRAPHICS ENVIRONMENT. *Computing in Science & Engineering*.

Isikdogan, F., Bovik, A., & Passalacqua, P. (2017). RivaMap: An automated river analysis and mapping engine. *Remote Sensing of Environment*, *202*, 88–97. https://doi.org/10.1016/j.rse.2017.03.044

Jerolmack, D. J. (2009). Conceptual framework for assessing the response of delta channel networks to Holocene sea level rise. *Quaternary Science Reviews*, *28*(17–18), 1786–1800. https://doi.org/10.1016/j.quascirev.2009.02.015

Jerolmack, D. J., & Swenson, J. B. (2007). Scaling relationships and evolution of distributary networks on wave-influenced deltas. *Geophysical Research Letters*, *34*(23), 2007GL031823. https://doi.org/10.1029/2007GL031823

Jones, L. S., & Schumm, S. A. (1999). Causes of Avulsion: An Overview. In N. D. Smith & J. Rogers (Eds.), *Fluvial Sedimentology VI* (1st ed., pp. 169–178). Wiley. https://doi.org/10.1002/9781444304213.ch13

Ke, W., Shaw, J. B., Mahon, R. C., & Cathcart, C. A. (2019). Distributary Channel Networks as Moving Boundaries: Causes and Morphodynamic Effects. *Journal of Geophysical Research: Earth Surface*, *124*(7), 1878–1898. https://doi.org/10.1029/2019JF005084

Kelly, S. B., & Olsen, H. (1993). Terminal fans a review with reference to Devonian examples. In *Sedimentary Geology* (Vol. 85, pp. 339–374).

Lauzon, R., Piliouras, A., & Rowland, J. C. (2019). Ice and Permafrost Effects on Delta Morphology and Channel Dynamics. *Geophysical Research Letters*, *46*(12), 6574–6582. https://doi.org/10.1029/2019GL082792

Leier, A. L., DeCelles, P. G., & Pelletier, J. D. (2005). Mountains, monsoons, and megafans. *Geology*, *33*(4), 289. https://doi.org/10.1130/G21228.1

Leonardi, N., Canestrelli, A., Sun, T., & Fagherazzi, S. (2013). Effect of tides on mouth bar morphology and hydrodynamics. *Journal of Geophysical Research: Oceans*, *118*(9), 4169–4183. https://doi.org/10.1002/jgrc.20302

Limaye, A. B., Adler, J. B., Moodie, A. J., Whipple, K. X., & Howard, A. D. (2023). Effect of Standing Water on Formation of Fan-Shaped Sedimentary Deposits at Hypanis Valles, Mars. *Geophysical Research Letters*, *50*(4), e2022GL102367. https://doi.org/10.1029/2022GL102367

Mahon, R., Hughes, C., Chen, H., & Shaw, J. (2024). Ancient Channel-Mouth Bifurcation Angles on Earth and Mars. *The Sedimentary Record*, *22*(1). https://doi.org/10.2110/001c.124824

Malin, M. C., & Edgett, K. S. (2015). *Evidence for Persistent Flow and Aqueous Sedimentation on Early Mars*. www.sciencemag.org

Martin, H. K., & Edmonds, D. A. (2023). Avulsion dynamics determine fluvial fan morphology in a cellular model. *Geology*, *51*(8), 796–800. https://doi.org/10.1130/G51138.1

Mendenhall, W., Beaver, R. J., & Beaver, B. M. (2012). *Introduction to Probability and Statistics*. Brooks/Cole.

Mohrig, D., Heller, P. L., Paola, C., & Lyons, W. J. (2000). Interpreting avulsion process from ancient alluvial sequences: Guadalope-Matarranya system (northern Spain) and Wasatch Formation (western Colorado). *Geological Society of America Bulletin*.

Morais, E. S., & Montanher, O. C. (2022). Avulsion in a meandering river: Floodplain conditions for occurrence and effects in the parent channel. *CATENA*, *214*, 106236. https://doi.org/10.1016/j.catena.2022.106236

Morón, S., Amos, K., Edmonds, D. A., Payenberg, T., Sun, X., & Thyer, M. (2017). Avulsion triggering by El Niño–Southern Oscillation and tectonic forcing: The case of the tropical Magdalena River, Colombia. *GSA Bulletin*, *129*(9–10), 1300–1313. https://doi.org/10.1130/B31580.1

Moscariello, A. (2018). Alluvial fans and fluvial fans at the margins of continental sedimentary basins: Geomorphic and sedimentological distinction for geo-energy exploration and development. *Geological Society, London, Special Publications*, *440*(1), 215–243. https://doi.org/10.1144/SP440.11

Nichols, G. J. (1987). *STRUCTURAL CONTROLS ON FLUVIAL DISTRIBUTARY SYSTEMS-THE LUNA SYSTEM, NORTHERN SPAIN*.

Nichols, G. J., & Fisher, J. A. (2007). Processes, facies and architecture of fluvial distributary system deposits. *Sedimentary Geology*, *195*(1–2), 75–90. https://doi.org/10.1016/j.sedgeo.2006.07.004

Nienhuis, J. H., Ashton, A. D., Edmonds, D. A., Hoitink, A. J. F., Kettner, A. J., Rowland, J. C., & Törnqvist, T. E. (2020). Global-scale human impact on delta morphology has led to net land area gain. *Nature*, *577*(7791), 514–518. https://doi.org/10.1038/s41586-019-1905-9

Nienhuis, J. H., Ashton, A. D., & Giosan, L. (2015). What makes a delta wave-dominated? *Geology*, *43*(6), 511–514. https://doi.org/10.1130/G36518.1

Nienhuis, J. H., Hoitink, A. J. F. T., & Törnqvist, T. E. (2018). Future Change to Tide-Influenced Deltas. *Geophysical Research Letters*, *45*(8), 3499–3507. https://doi.org/10.1029/2018GL077638

North, C. P., & Warwick, G. L. (2007). Fluvial Fans: Myths, Misconceptions, and the End of the Terminal-Fan Model. *Journal of Sedimentary Research*, *77*(9), 693–701. https://doi.org/10.2110/jsr.2007.072

Olariu, C., & Bhattacharya, J. P. (2006). Terminal distributary channels and delta front architecture of river-dominated delta systems. *Journal of Sedimentary Research*, *76*(2), 212–233. https://doi.org/10.2110/jsr.2006.026

Ori, G. G., Marinangeli, L., & Baliva, A. (2000). Terraces and Gilbert-type deltas in crater lakes in Ismenius Lacus and Memnonia (Mars). *Journal of Geophysical Research: Planets*, *105*(E7), 17629–17641. https://doi.org/10.1029/1999JE001219

Owen, A., Nichols, G. J., Hartley, A. J., Weissmann, G. S., & Scuderi, L. A. (2015). Quantification of a Distributive Fluvial System: The Salt Wash DFS of the Morrison Formation, SW U.S.A. *Journal of Sedimentary Research*, *85*(5), 544–561. https://doi.org/10.2110/jsr.2015.35

985 Paniagua-Arroyave, J. F., & Nienhuis, J. H. (2024). The Quantified Galloway Ternary Diagram of Delta
986 Morphology. *Journal of Geophysical Research: Earth Surface*, *129*(11), e2024JF007878.
987 https://doi.org/10.1029/2024JF007878

988 Paola, C., Twilley, R. R., Edmonds, D. A., Kim, W., Mohrig, D., Parker, G., Viparelli, E., & Voller, V. R.
989 (2011). Natural Processes in Delta Restoration: Application to the Mississippi Delta. *Annual Review of*
990 *Marine Science*, *3*(1), 67–91. https://doi.org/10.1146/annurev-marine-120709-142856

991 Parker, G., Paola, C., Whipple, K. X., & Mohrig, D. (1998). ALLUVIAL FANS FORMED BY CHANNELIZED
992 FLUVIAL AND SHEET FLOW. I: THEORY. *Jounral OF Hydraulic Engineering*, 985–995.

993 Passalacqua, P. (2017). The Delta Connectome: A network-based framework for studying connectivity in
994 river deltas. *Geomorphology*, *277*, 50–62. https://doi.org/10.1016/j.geomorph.2016.04.001

995 Pearson, S. G., Van Prooijen, B. C., Elias, E. P. L., Vitousek, S., & Wang, Z. B. (2020). Sediment
996 Connectivity: A Framework for Analyzing Coastal Sediment Transport Pathways. *Journal of Geophysical*
997 *Research: Earth Surface*, *125*(10), e2020JF005595. https://doi.org/10.1029/2020JF005595

998 Piliouras, A., Lauzon, R., & Rowland, J. C. (2021). Unraveling the Combined Effects of Ice and Permafrost
999 on Arctic Delta Morphodynamics. *Journal of Geophysical Research: Earth Surface*, *126*(4),
1000 e2020JF005706. https://doi.org/10.1029/2020JF005706

1001 Pizzuto, J. E. (1987). Sediment diffusion during overbank flows. *Sedimentology*, *34*(2), 301–317.
1002 https://doi.org/10.1111/j.1365-3091.1987.tb00779.x

1003 Plink-Björklund, P. (2021). Distributive Fluvial Systems: Fluvial and Alluvial Fans. In *Encyclopedia of*
1004 *Geology* (pp. 745–758). Elsevier. https://doi.org/10.1016/B978-0-08-102908-4.00015-1

1005 Radebaugh, J., Ventra, D., Lorenz, R. D., Farr, T., Kirk, R., Hayes, A., Malaska, M. J., Birch, S., Liu, Z. Y.-C.,
1006 Lunine, J., Barnes, J., Le Gall, A., Lopes, R., Stofan, E., Wall, S., & Paillou, P. (2018). Alluvial and fluvial fans
1007 on Saturn's moon Titan reveal processes, materials and regional geology. *Geological Society, London,*
1008 *Special Publications*, *440*(1), 281–305. https://doi.org/10.1144/SP440.6

1009 Rahman, M. M., Howell, J. A., & MacDonald, D. I. M. (2022). Quantitative analysis of crevasse-splay
1010 systems from modern fluvial settings. *Journal of Sedimentary Research*, *92*(9), 751–774.
1011 https://doi.org/10.2110/jsr.2020.067

1012 Reitz, M. D., & Jerolmack, D. J. (2012). Experimental alluvial fan evolution: Channel dynamics, slope
1013 controls, and shoreline growth. *Journal of Geophysical Research: Earth Surface*, *117*(F2), 2011JF002261.
1014 https://doi.org/10.1029/2011JF002261

1015 Saito, Y., Thanawat, J., Chaimanee, N., Jarupongsakul, T., & Syvitski, J. P. M. (2007). *Shrinking*
1016 *Megadeltas in Asia: Sea-level Rise and Sediment Reduction Impacts from Case Study of the Chao Phraya*
1017 *Delta The Holocene Red River Delta, Vietnam View project Global Risks and research priorities for coastal*
1018 *subsidence View project Shrinking Megadeltas in Asia: Sea-level Rise and Sediment Reduction Impacts*
1019 *from Case Study of the Chao Phraya Delta*. https://www.researchgate.net/publication/234045413

1020 Schumm, S. A. (1977). The fluvial system. *Food and Agriculture Organization of the United Nations*.

1021 Schwanghart, W., & Kuhn, N. J. (2010). TopoToolbox: A set of Matlab functions for topographic analysis.
1022 *Environmental Modelling & Software*, *25*(6), 770–781. https://doi.org/10.1016/j.envsoft.2009.12.002

1023 Seybold, H., Andrade, J. S., & Herrmann, H. J. (2007). Modeling river delta formation. *Proceedings of the*
1024 *National Academy of Sciences*, *104*(43), 16804–16809. https://doi.org/10.1073/pnas.0705265104

1025 Seybold, H. J., Kite, E., & Kirchner, J. W. (2018). Branching geometry of valley networks on Mars and
1026 Earth and its implications for early Martian climate. *Science Advances*, *4*(6), eaar6692.
1027 https://doi.org/10.1126/sciadv.aar6692

1028 Seybold, H., Rothman, D. H., & Kirchner, J. W. (2017). Climate's watermark in the geometry of stream
1029 networks. *Geophysical Research Letters*, *44*(5), 2272–2280. https://doi.org/10.1002/2016GL072089

1030 Shaw, J. B., Miller, K., & McElroy, B. (2018). Island Formation Resulting From Radially Symmetric Flow
1031 Expansion. *Journal of Geophysical Research: Earth Surface*, *123*(2), 363–383.
1032 https://doi.org/10.1002/2017JF004464

1033 Singh, H., Parkash, B., & Gohain, K. (1993). Facies analysis of the Kosi megafan deposits. *Sedimentary*
1034 *Geology*, *85*(1–4), 87–113. https://doi.org/10.1016/0037-0738(93)90077-I

1035 Sinha, R. (2009). The Great avulsion of Kosi on 18 August 2008. *Current Science*, *97*(3), 429–433.

1036 Slingerland, R., & Smith, N. D. (1998). Necessary conditions for a meandering-river avulsion. *Geology*,
1037 *26*(5), 435. https://doi.org/10.1130/0091-7613(1998)026%253C0435:NCFAMR%253E2.3.CO;2

1038 Slingerland, R., & Smith, N. D. (2004). RIVER AVULSIONS AND THEIR DEPOSITS. *Annual Review of Earth*
1039 *and Planetary Sciences*, *32*(1), 257–285. https://doi.org/10.1146/annurev.earth.32.101802.120201

1040 Smart, J. S. (1971). *QUANTITATIVE PROPERTIES OF DELTA CHANNEL NETWORKS*.

1041 Syvitski, J. P. M., & Brakenridge, G. R. (2013). Causation and avoidance of catastrophic flooding along the
1042 Indus River, Pakistan. *GSA Today*, *23*(1), 4–10. https://doi.org/10.1130/GSATG165A.1

1043 Syvitski, J. P. M., Kettner, A. J., Overeem, I., Hutton, E. W. H., Hannon, M. T., Brakenridge, G. R., Day, J.,
1044 Vörösmarty, C., Saito, Y., Giosan, L., & Nicholls, R. J. (2009). Sinking deltas due to human activities.
1045 *Nature Geoscience*, *2*(10), 681–686. https://doi.org/10.1038/ngeo629

1046 Tebolt, M., & Goudge, T. A. (2022). Global investigation of martian sedimentary fan features: Using
1047 stratigraphic analysis to study depositional environment. *Icarus*, *372*, 114718.
1048 https://doi.org/10.1016/j.icarus.2021.114718

1049 Tejedor, A., Longjas, A., Edmonds, D. A., Zaliapin, I., Georgiou, T. T., Rinaldo, A., & Foufoula-Georgiou, E.
1050 (2017). Entropy and optimality in river deltas. *Proceedings of the National Academy of Sciences*, *114*(44),
1051 11651–11656. https://doi.org/10.1073/pnas.1708404114

1052 Tejedor, A., Longjas, A., Zaliapin, I., & Foufoula-Georgiou, E. (2015). Delta channel networks: 1. A graph-
1053 theoretic approach for studying connectivity and steady state transport on deltaic surfaces. *Water*
1054 *Resources Research*, *51*(6), 3998–4018. https://doi.org/10.1002/2014WR016577

1055 Törnqvist, T. E., & Bridge, J. S. (2002). Spatial variation of overbank aggradation rate and its influence on
1056 avulsion frequency. *Sedimentology*, *49*(5), 891–905. https://doi.org/10.1046/j.1365-3091.2002.00478.x

Trampush, S. M., & Hajek, E. A. (2017). Preserving proxy records in dynamic landscapes: Modeling and examples from the Paleocene-Eocene Thermal Maximum. *Geology*, *45*(11), 967–970. https://doi.org/10.1130/G39367.1

Trauth, M. H. (2006). *MATLAB ® Recipes for Earth Sciences*.

Ventra, D., & Clarke, L. E. (2018). Geology and geomorphology of alluvial and fluvial fans: Current progress and research perspectives. *Geological Society, London, Special Publications*, *440*(1), 1–21. https://doi.org/10.1144/SP440.16

Virtanen, P., Gommers, R., Oliphant, T. E., Haberland, M., Reddy, T., Cournapeau, D., Burovski, E., Peterson, P., Weckesser, W., Bright, J., van der Walt, S. J., Brett, M., Wilson, J., Millman, K. J., Mayorov, N., Nelson, A. R. J., Jones, E., Kern, R., Larson, E., … Vázquez-Baeza, Y. (2020). SciPy 1.0: Fundamental algorithms for scientific computing in Python. *Nature Methods*, *17*(3), 261–272. https://doi.org/10.1038/s41592-019-0686-2

Vulis, L., Tejedor, A., Ma, H., Nienhuis, J. H., Broaddus, C. M., Brown, J., Edmonds, D. A., Rowland, J. C., & Foufoula-Georgiou, E. (2023). River Delta Morphotypes Emerge From Multiscale Characterization of Shorelines. *Geophysical Research Letters*, *50*(7), e2022GL102684. https://doi.org/10.1029/2022GL102684

Walker, H. J. (1998). Arctic Deltas. *Journal of Coastal Research*, *14*(3), 718–738.

Wall, S., Hayes, A., Bristow, C., Lorenz, R., Stofan, E., Lunine, J., Le Gall, A., Janssen, M., Lopes, R., Wye, L., Soderblom, L., Paillou, P., Aharonson, O., Zebker, H., Farr, T., Mitri, G., Kirk, R., Mitchell, K., Notarnicola, C., … Ventura, B. (2010). Active shoreline of Ontario Lacus, Titan: A morphological study of the lake and its surroundings. *Geophysical Research Letters*, *37*(5), 2009GL041821. https://doi.org/10.1029/2009GL041821

Wang, J., & Plink-Björklund, P. (2019). Stratigraphic complexity in fluvial fans: Lower Eocene Green River Formation, Uinta Basin, USA. *Basin Research*, *31*(5), 892–919. https://doi.org/10.1111/bre.12350

Waskom, M. (2021). seaborn: Statistical data visualization. *Journal of Open Source Software*, *6*(60), 3021. https://doi.org/10.21105/joss.03021

Weissman, G. S., Hartley, A. J., Nichols, G. J., Scuderi, L. A., Olson, M., Buehler, H., & Banteah, R. (2010). *Fluvial form in modern continental sedimentary basins: Distributive fluvial systems*. https://doi.org/10.1016/j.geo

Weissmann, G. S., Hartley, A. J., Nichols, G. J., Scuderi, L. A., Olson, M., Buehler, H., & Banteah, R. (2010). Fluvial form in modern continental sedimentary basins: Distributive fluvial systems. *Geology*, *38*(1), 39–42. https://doi.org/10.1130/G30242.1

Weissmann, G. S., Hartley, A. J., Scuderi, L. A., Nichols, G. J., Owen, A., Wright, S., Felicia, A. L., Holland, F., & Anaya, F. M. L. (2015). Fluvial geomorphic elements in modern sedimentary basins and their potential preservation in the rock record: A review. *Geomorphology*, *250*, 187–219. https://doi.org/10.1016/j.geomorph.2015.09.005

Witek, P. P., & Czechowski, L. (2015). Dynamical modelling of river deltas on Titan and Earth. *Planetary and Space Science*, *105*, 65–79. https://doi.org/10.1016/j.pss.2014.11.005

Wolinsky, M. A., Edmonds, D. A., Martin, J., & Paola, C. (2010). Delta allometry: Growth laws for river deltas. *Geophysical Research Letters*, *37*(21), 2010GL044592. https://doi.org/10.1029/2010GL044592

Wood, L. J. (2006). Quantitative geomorphology of the Mars Eberswalde delta. *Geological Society of America Bulletin*, *118*(5–6), 557–566. https://doi.org/10.1130/B25822.1

Wright, L. D. (1977). Sediment transport and deposition at river mouths: A synthesis. *Geological Society of America Bulletin*, *88*(6), 857. https://doi.org/10.1130/0016-7606(1977)88%253C857:STADAR%253E2.0.CO;2

Xu, Z., & Plink-Björklund, P. (2023). Quantifying Formative Processes in River- and Tide-Dominated Deltas for Accurate Prediction of Future Change. *Geophysical Research Letters*, *50*(20), e2023GL104434. https://doi.org/10.1029/2023GL104434

Yang, H. (2020). Numerical investigation of avulsions in gravel-bed braided rivers. *Hydrological Processes*, *34*(17), 3702–3717. https://doi.org/10.1002/hyp.13837